Mouri A, Noda Y, Enomoto T, Nabeshima T (2007a) Phencyclidine animal models of schizophrenia: approaches from abnormality of glutamatergic neurotransmission and neurodevelopment. Neurochem Int 51:173–184

Mouri A, Noda Y, Noda A, Nakamura T, Tokura T, Yura Y, Nitta A, Furukawa H, Nabeshima T (2007b) Involvement of a dysfunctional dopamine-D1/*N*-methyl-d-aspartate-NR1 and Ca^{2+}/calmodulin-dependent protein kinase II pathway in the impairment of latent learning in a model of schizophrenia induced by phencyclidine. Mol Pharmacol 71:1598–1609

Murai R, Noda Y, Matsui K, Kamei H, Mouri A, Matsuba K, Nitta A, Furukawa H, Nabeshima T (2007) Hypofunctional glutamatergic neurotransmission in the prefrontal cortex is involved in the emotional deficit induced by repeated treatment with phencyclidine in mice: implications for abnormalities of glutamate release and NMDA-CaMKII signaling. Behav Brain Res 180:152–160

Nagai T, Yamada K, Kim HC, Kim YS, Noda Y, Imura A, Nabeshima Y, Nabeshima T (2003) Cognition impairment in the genetic model of aging klotho gene mutant mice: a role of oxidative stress. FASEB J 17:50–52

Nagai T, Takuma K, Kamei H, Ito Y, Nakamichi N, Ibi D, Nakanishi Y, Murai M, Mizoguchi H, Nabeshima T, Yamada K (2007) Dopamine D1 receptors regulate protein synthesis-dependent long-term recognition memory via extracellular signal-regulated kinase 1/2 in the prefrontal cortex. Learn Mem 14:117–125

Newcomer JW (2005) Second-generation (atypical) antipsychotics and metabolic effects: a comprehensive literature review. CNS Drugs 19(Suppl 1):1–93

Newman-Tancredi A, Verriele L, Touzard M, Millan MJ (2001) Efficacy of antipsychotic agents at human 5-HT1A receptors determined by [^{3}H]WAY100,635 binding affinity ratios: relationship to efficacy for G-protein activation. Eur J Pharmacol 428:177–184

Noda Y, Yamada K, Furukawa H, Nabeshima T (1995) Enhancement of immobility in a forced swimming test by subacute or repeated treatment with phencyclidine: a new model of schizophrenia. Br J Pharmacol 116:2531–2537

Noda Y, Mamiya T, Furukawa H, Nabeshima T (1997) Effects of antidepressants on phencyclidine-induced enhancement of immobility in a forced swimming test in mice. Eur J Pharmacol 324:135–140

Noda Y, Kamei H, Mamiya T, Furukawa H, Nabeshima T (2000) Repeated phencyclidine treatment induces negative symptom-like behavior in forced swimming test in mice: imbalance of prefrontal serotonergic and dopaminergic functions. Neuropsychopharmacology 23:375–387

Nuechterlein KH, Barch DM, Gold JM, Goldberg TE, Green MF, Heaton RK (2004) Identification of separable cognitive factors in schizophrenia. Schizophr Res 72:29–39

Pearlson GD (2000) Neurobiology of schizophrenia. Ann Neurol 48:556–566

Qiao H, Noda Y, Kamei H, Nagai T, Furukawa H, Miura H, Kayukawa Y, Ohta T, Nabeshima T (2001) Clozapine, but not haloperidol, reverses social behavior deficit in mice during withdrawal from chronic phencyclidine treatment. Neuroreport 12:11–15

Rainey Jr JM, Crowder MK (1975) Prolonged psychosis attributed to phencyclidine: report of three cases. Am J Psychiatry 132:1076–1078

Rivas-Vasquez RA (2003) Aripiprazole: a novel antipsychotic with dopamine-stabilising properties. Prof Psychol: Res Prac 34:108–111

Rollema H, Lu Y, Schmidt AW, Sprouse JS, Zorn SH (2000) 5-HT1A receptor activation contributes to ziprasidone-induced dopamine release in the rat prefrontal cortex. Biol Psychiatry 48:229–237

Rössler W, Salize HJ, van Os J, Riecher-Rössler A (2005) Size of burden of schizophrenia and psychotic disorders. Eur Neuropsychopharmacol 15:399–409

Sawaguchi T, Goldman-Rakic PS (1991) D1 dopamine receptors in prefrontal cortex: involvement in working memory. Science 251:947–950

Shapiro DA, Renock S, Arrington E, Chiodo LA, Liu LX, Sibley DR, Roth BL, Mailman R (2003) Aripiprazole, a novel atypical antipsychotic drug with a unique and robust pharmacology. Neuropsychopharmacology 28:1400–1411

Shimokawa Y, Akiyama H, Kashiyama E, Koga T, Miyamoto G (2005) High performance liquid chromatographic methods for the determination of aripiprazole with ultraviolet detection in rat plasma and brain: application to the pharmacokinetic study. J Chromatogr B Analyt Technol Biomed Life Sci 821:8–14

Sprouse JS, Reynolds LS, Braselton JP, Rollema H, Zorn SH (1999) Comparison of the novel antipsychotic ziprasidone with clozapine and olanzapine: inhibition of dorsal raphe cell firing and the role of 5-HT1A receptor activation. Neuropsychopharmacol 21:622–631

Stark AD, Jordan S, Allers KA, Bertekap RL, Chen R, Mistry Kannan T, Molski TF, Yocca FD, Sharp T, Kikuchi T, Burris KD (2007) Interaction of the novel antipsychotic aripiprazole with 5-HT1A and 5-HT 2A receptors: functional receptor-binding and in vivo electrophysiological studies. Psychopharmacology 190:373–382

Sumiyoshi T, Matsui M, Nohara S, Yamashita I, Kurachi M, Sumiyoshi C, Jayathilake K, Meltzer HY (2001a) Enhancement of cognitive performance in schizophrenia by addition of tandospirone to neuroleptic treatment. Am J Psychiatry 158:1722–1725

Sumiyoshi T, Matsui M, Yamashita I, Nohara S, Kurachi M, Uehara T, Sumiyoshi S, Sumiyoshi C, Meltzer HY (2001b) The effect of tandospirone, a serotonin-1A agonist, on memory function in schizophrenia. Biol Psychiatry 49:861–868

Tamminga CA (2002) Partial dopamine agonists in the treatment of psychosis. J Neural Transm 109:411–420

Tamminga CA (2006) The neurobiology of cognition in schizophrenia. J Clin Psychiatry 67:9–13

Tan HY, Callicott JH, Weinberger DR (2007) Dysfunctional and compensatory prefrontal cortical systems, genes and the pathogenesis of schizophrenia. Cereb Cortex 17:i171–i181

Tang YP, Shimizu E, Dube GR, Rampon C, Kerchner GA, Zhuo M, Liu G, Tsien JZ (1999) Genetic enhancement of learning and memory in mice. Nature 401:63–69

Vincent SL, Khan Y, Benes FM (1995) Cellular colocalization of dopamine D1 and D2 receptors in rat medial prefrontal cortex. Synapse 19:112–120

Woodward ND, Purdon SE, Meltzer HY, Zald DH (2005) A meta-analysis of neuropsychological change to clozapine, olanzapine, quetiapine, and risperidone in schizophrenia. Int J Neuropsychopharmacol 8:457–472

Zocchi A, Fabbri D, Heidbreder CA (2005) Aripiprazole increases dopamine but not noradrenaline and serotonin levels in the mouse prefrontal cortex. Neurosci Lett 387:157–161

nature genetics

Usp46 is a quantitative trait gene regulating mouse immobile behavior in the tail suspension and forced swimming tests

Shigeru Tomida[1], Takayoshi Mamiya[2], Hirotake Sakamaki[1], Masami Miura[3], Toshihiko Aosaki[3], Masao Masuda[3], Minae Niwa[2], Tsutomu Kameyama[4], Junya Kobayashi[1], Yuka Iwaki[1], Saki Imai[1], Akira Ishikawa[5], Kuniya Abe[6], Takashi Yoshimura[1], Toshitaka Nabeshima[2] & Shizufumi Ebihara[1]

The tail suspension test (TST) and forced swimming test (FST) are widely used for assessing antidepressant activity and depression-like behavior. We found that CS mice show negligible immobility in inescapable situations. Quantitative trait locus (QTL) mapping using CS and C57BL/6J mice revealed significant QTLs on chromosomes 4 (FST) and 5 (TST and FST). To identify the quantitative trait gene on chromosome 5, we narrowed the QTL interval to 0.5 Mb using several congenic and subcongenic strains. Ubiquitin-specific peptidase 46 (*Usp46*) with a lysine codon deletion was located in this region. This deletion affected nest building, muscimol-induced righting reflex and anti-immobility effects of imipramine. The muscimol-induced current in the hippocampal CA1 pyramidal neurons and hippocampal expression of the 67-kDa isoform of glutamic acid decarboxylase were significantly decreased in the *Usp46* mutant mice compared to control mice. These phenotypes were rescued in transgenic mice with bacterial artificial chromosomes containing wild-type *Usp46*. Thus, *Usp46* affects the immobility in the TST and FST, and it is implicated in the regulation of GABA action.

The TST and FST have been recognized as useful experimental paradigms for assessing antidepressant activity and depression-like behavior. In these tests, animals are subjected to the short-term, inescapable stress of being suspended by their tail or being forced to swim in a water-filled cylinder. In such situations, the animals rapidly adopt a characteristic immobile posture that has been named "behavioral despair" on the assumption that the animals have given up hope of escaping[1,2]. These tests have been widely used for screening drugs for antidepressant activity and in preclinical depression studies for understanding the underlying pathophysiology of affective disorders, particularly for assessing depression-related behavior in genetically modified mice[3,4].

Several mental illnesses such as affective disorders or schizophrenia are thought to arise from naturally occurring variant genes and their interactions, and from gene-environment interactions in which each gene confers subtle effects on the appearance of the diseases. In the absence of such interactions, the disease risk elicited by each variant gene is low but increases with an appropriate combination of genetic and environmental factors. Because diseases elicited by single gene defects are fairly rare, QTL analysis has been extensively performed in animal models to dissect such complex traits[5]. However, these attempts have hardly been successful, and $<1\%$ of QTLs (only approximately 20 genes) have been identified in mice and rats[6]. In recent years, several QTL studies have been conducted in mice on the basal immobility time and antidepressant response in the TST and FST[7–11]. These studies have resulted in the mapping of many QTLs, and several candidate genes underlying these behaviors have been proposed; however, so far investigators have not identified any genes as responsible for these behaviors.

The CS mouse is an inbred strain originally established by the hybridization of the NBC and SII strains, which are both now extinct. CS mice exhibit several distinct phenotypes of circadian behavioral rhythms, such as a long free-running period, spontaneous rhythm splitting and entrainment of circadian rhythms in response to a daily restricted feeding schedule under constant darkness[12–14]. In addition, the sleep properties of CS mice are distinct from those of C57BL/6J and C3H/He mice, which have normal circadian rhythms[15]. Because many mental illnesses are associated with abnormalities in the circadian system and sleep patterns, we characterized the behavioral phenotypes in CS mice with a battery of behavioral tests. Among these phenotypes, we found that CS mice show an extremely low immobility time (almost no immobility) in both the TST and FST, which

[1]Division of Biomodeling, Graduate School of Bioagricultural Sciences, Nagoya University, Furo-cho, Chikusa-ku, Nagoya, Japan. [2]Department of Chemical Pharmacology, Faculty of Pharmacy, Meijo University, Tempaku-ku, Nagoya, Japan. [3]Neural Circuits Dynamics Research Group, Tokyo Metropolitan Institute of Gerontology, Itabashi-ku, Tokyo, Japan. [4]Japan Institute of Psychopharmacology, Higashi-ku, Nagoya, Japan. [5]Division of Applied Genetics and Physiology, Graduate School of Bioagricultural Sciences, Nagoya University, Furo-cho, Chikusa-ku, Nagoya, Japan. [6]RIKEN BioResource Center, Technology and Development Team for Mammalian Cellular Dynamics, Tsukuba, Japan. Correspondence should be addressed to S.E. (ebihara@agr.nagoya-u.ac.jp).

Received 10 June 2008; accepted 2 February 2009; published online 24 May 2009; doi:10.1038/ng.344

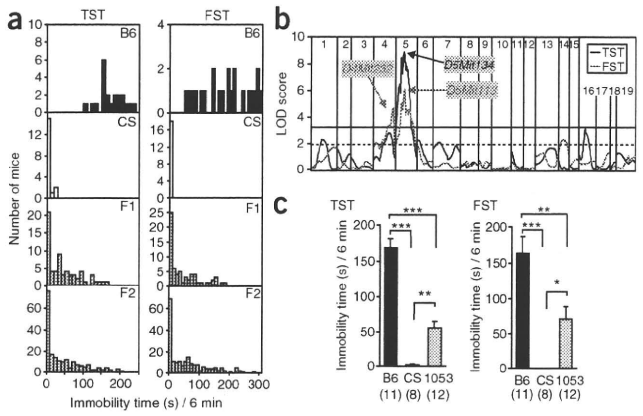

Figure 1 Linkage analysis and phenotypes of the chromosome 5 congenic strain. (**a**) Frequency histograms of the immobility time in the tail suspension test (TST) and the forced swimming test (FST) for parental, F_1 and F_2 mice. (**b**) Genome-wide linkage analysis for the immobility time on TST and FST using Map Manager QTXb20. Three significant QTLs were mapped with a peak at *D5Mit134* on TST and at *D4Mit232* and *D5Mit113* on FST. The solid and dotted lines indicate the significance level (LOD score = 3.30 on both TST and FST) and suggestive level (LOD score = 1.95 on both TST and FST), respectively. (**c**) TST and FST immobility time (mean ± s.e.m.) in B6, CS and B6.CS-Ngu1053 male mice. The CS and B6.CS-Ngu1053 mice showed a significantly shorter immobility time than the B6 mice on both TST and FST (one-way ANOVA: TST, $F_{2,28} = 46.3$, $P < 9.4 \times 10^{-10}$; FST, $F_{2,28} = 18.8$, $P < 6.6 \times 10^{-6}$; Tukey-Kramer *post hoc* test: $^{***}P < 0.001$, $^{**}P < 0.01$, $^{*}P < 0.05$). The number of mice used is shown within parentheses.

prompted us to undertake QTL genetic analysis to identify the responsible gene. By using a forward genetic approach[6,16,17], we succeeded in identifying the responsible gene. Here, we report that the gene encoding ubiquitin-specific peptidase 46 (*Usp46*) is one of the quantitative trait genes that cause such behaviors.

RESULTS

Behavioral phenotyping of the C57BL/6J and CS strains

To assess the behavioral characteristics of the CS strain, we subjected C57BL/6J (B6) and CS mice to a battery of behavioral tests, including the open-field, light-dark exploration, elevated plus-maze, prepulse inhibition, Y-maze, tail suspension and forced swimming tests (**Supplementary Table 1** online).

The open-field test is widely used to quantitate overall activity and anxiety-related behavior, although this test is not so specific for anxiety-related behavior[18]. In this test, the ambulatory activity was significantly lower in the CS mice than in the B6 mice ($P < 0.01$, Student's *t*-test), but no differences were observed in the other phenotypes (grooming, rearing and defecation). In the light-dark box test, which is primarily used to detect anxiolytic-like or anxiogenic-like activity of a drug[19], the CS mice spent significantly less time ($P < 0.01$, Student's *t*-test) in the dark compartment and defecated more frequently ($P < 0.01$, Mann-Whitney *U* test) than the B6 mice, although there were no significant differences in the time of light-dark transitions between the two compartments. In the elevated plus-maze test, which is also used to detect anxiolytic-like behavior[20], no significant differences were observed in the time spent on the open arm between the two strains; however, the CS mice defecated more frequently ($P < 0.001$, Student's *t*-test) than the B6 mice. The prepulse inhibition test, in which a weak prestimulus or prepulse suppresses the response to a startling stimulus, is used to evaluate sensorimotor gating, and it is thought that deficits in this response represent biological markers for schizophrenia[20,21]. In this test and in the Y-maze test, which is considered to reflect the status of short-term and working memory in humans[22], there were no significant differences between the two strains. In contrast to the above-mentioned phenotypes, the results in the TST and FST were unusual in the CS mice, which showed negligible immobility throughout the test period.

QTL analysis

To map the genes responsible for the aberrant immobility of CS mice observed in the TST and FST, we genotyped 203 F_2 mice produced by intercrossing F_1 mice obtained from B6 and CS mice; interval mapping was performed using Map Manager QTXb20 followed by nonparametric interval mapping using R/qtl (http://www.rqtl.org/). Consequently, we detected significant QTLs in the TST (likelihood of odds score (LOD) 8.90, QTXb20; LOD 8.92, R/qtl) and FST (LOD 6.08, QTXb20; LOD 6.92, R/qtl) on chromosome 5, and only in the FST (LOD 4.71, QTXb20; LOD 4.09, R/qtl) on chromosome 4 (**Fig. 1a,b**; **Supplementary Fig. 1** and **Supplementary Tables 2** and **3** online). The peak positions of the QTLs on chromosome 5 for immobility in the TST and FST were similar (TST: 29 cM for QTXb20, 28 cM for R/qtl; FST: 30 cM for QTXb20, 30 cM for R/qtl). In addition, suggestive QTLs were detected on chromosomes 1, 4, 6, 7 and 16 in the TST and on chromosome 14 in the FST by QTXb20, and on chromosomes 4, 6, 7 and 16 in the TST and on chromosomes 1, 6 and 14 in the FST by R/qtl (**Supplementary Tables 2** and **3**). To detect epistatic interactions, we performed two-locus interaction analysis for all possible markers using QTXb20. However, we could not find any pair of markers that significantly affected the immobility time in the TST and FST ($P > 0.05$).

Reducing the QTL interval

To reduce the QTL interval on chromosome 5, we developed a number of congenic or subcongenic strains by crossing CS as the donor strain with B6 as the recipient strain using a "speed-congenic" approach (**Supplementary Fig. 2** online). The B6.CS-Ngu1053 strain, which was subsequently used in different experiments, carried homozygous CS alleles within its congenic interval (an approximately 16-Mb region from *D5B6CS85* to *D5Mit259*) on a B6 genetic background. To validate QTL linkage analysis, we subjected the B6.CS-Ngu1053 strain to TST and FST and found that the immobility time of this strain was significantly shorter than that of the B6 strain in both the TST and the FST; however, its immobility time was longer than that of CS in both the tests (TST: $P < 0.001$ versus B6, $P < 0.01$ versus CS; FST: $P < 0.01$ versus B6, $P < 0.05$ versus CS) (**Fig. 1c**).

To narrow down the critical interval that harbors the responsible gene, we generated two subcongenic strains by crossing B6.CS-Ngu1053 with B6. The B6.CS-Ngu2271 strain contained an approximately 0.5-Mb nonoverlapping region with the B6.CS-Ngu1053 strain at the centromeric side, whereas the B6.CS-Ngu3042 strain carried a nonoverlapping region at the telomeric side (**Fig. 2a**). The B6.CS-Ngu2271 strain showed almost the same TST immobility time as B6, which indicates that the 0.5-Mb nonoverlapping region represents the critical interval. The shorter immobility time of the B6.CS-Ngu3042 strain supports the notion that the responsible quantitative trait gene is located in this interval.

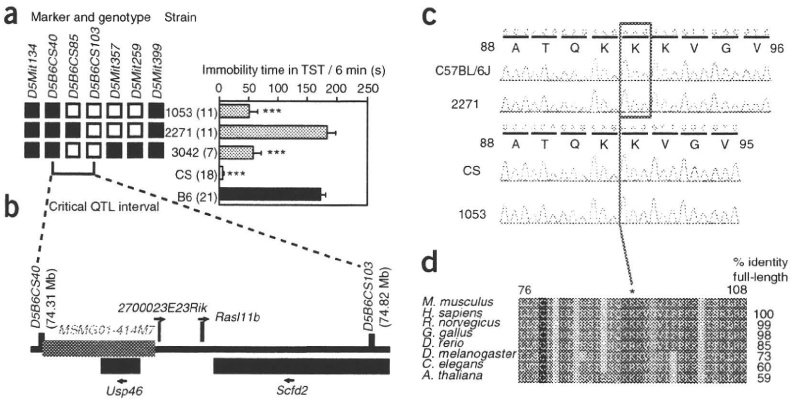

Figure 2 Identifying the quantitative trait gene on mouse chromosome 5 that influences TST immobility time. (**a**) Genotype and the immobility time on TST in the B6.CS-Ngu1053 (1053), B6.CS-Ngu2271 (2271) and B6.CS-Ngu3042 (3042) strains that define the critical QTL interval. The solid and open boxes represent the B6 and CS alleles, respectively, and 1053, 3042 and CS showed a significantly shorter immobility time than B6 (one-way ANOVA, $F_{4,63} = 81.8$, $P < 9.4 \times 10^{-10}$; Tukey-Kramer *post hoc* test, $^{***}P < 0.001$). The number of mice used is shown within parentheses. (**b**) The genes in the critical QTL interval and the BAC clone (*MSMG01-414M7*) used for transgenic rescue. The arrows indicate the directions of transcription. (**c**) The 3-bp deletion coding for lysine in the open reading frame of *Usp46* in CS and 1053. (**d**) The alignment of the amino acid sequences of the *Usp46* homologs. The region around the deletion of the lysine residue is highly conserved in different species. The sequence identity for the full-length protein is shown. Mouse, NP_808229; human, NP_073743; rat, XP_214034; chicken, XP_420711; zebrafish, NP_001077025; fruitfly, NP_732801; *C. elegans*, P34547; *Arabidopsis*, NP_565532.

Candidate gene screening

The above-mentioned critical interval contained four or three genes and one expressed sequence tag (EST) gene (*Usp46*, *Rasl11b* and *2700023E23Rik* have been registered as genes in the National Center for Biotechnology Information (NCBI) database; *Scfd2* is located outside the interval as per the NCBI database; *Scfd2* is included in the interval and *1700112M01Rik* is designated as an EST gene in the Ensembl database) (**Fig. 2b**). To identify the responsible gene, we examined the sequence of the coding region of these genes and their expression in the brain by *in situ* hybridization and compared the sequences and gene expression among the B6, CS and B6.CS-Ngu1053 strains (**Supplementary Fig. 3** online). The result revealed only one 3-bp deletion (a lysine codon) in *Usp46* (**Fig. 2c,d**). We found no other differences in the expression sites or levels of this gene. The other genes apparently did not differ in their sequences, expression sites or levels among the three strains (**Supplementary Fig. 3**).

Analysis of transgenic strains

We produced transgenic and nontransgenic progeny with homozygous and heterozygous genotypes (**Fig. 3a**). Southern blot analysis revealed that the bacterial artificial chromosome (BAC) was integrated into the genomes of the founder mice (**Supplementary Fig. 4** online). To confirm *Usp46* transgene expression, we first sequenced the coding region of *Usp46* and detected the single nucleotide polymorphism (SNP) that differed between the MSM/Ms strain and the other two strains (B6 and CS). Using this SNP, we examined mRNA expression in the brains of the transgenic mice with B6 and CS heterozygous alleles (B/C) in the congenic region of the B6.CS-Ngu1053 strain and detected two signals derived from the endogenous allele (B6 and CS) and the transgene (MSM/Ms) (**Fig. 3b**; **Supplementary Fig. 5a** online), which indicated that *Usp46* was expressed in the brains of the transgenic mice. In addition, we investigated *Usp46* expression in the brain by *in situ* hybridization (**Fig. 3c**; **Supplementary Fig. 5b**). *Usp46* was strongly expressed in a number of regions, including the olfactory bulb, cingulum bundle, amygdala, hippocampus and cerebellum in the transgenic strains, although these strains showed different expression levels. As compared with the nontransgenic mice, there were no obvious regional differences in *Usp46* expression.

The *Usp46* transgene (tg) completely rescued the phenotype in both heterozygous (B/C) and CS homozygous (C/C) genotypes; however,

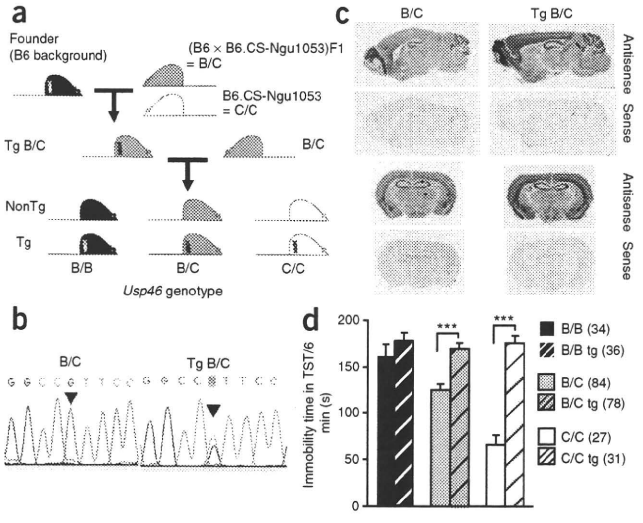

Figure 3 Generations and analysis of BAC transgenic mice. (**a**) The genetic cross used to produce the transgenic F_2 mice. The black, gray and white mice represent the B6 homozygous (B/B), B6 and CS heterozygous (B/C) and the CS homozygous allele (C/C) at the congenic region of the B6.CS-Ngu1053 strain, respectively. The presence of the transgene is indicated by a double helix symbol. Each congenic genotype (B/B, B/C and C/C) was combined with (tg) or without (non tg) the transgene. (**b**) The *Usp46* variant sites are indicated by an arrowhead (B6 and CS, guanine; MSM/Ms, adenine). The SNP is silent and located in exon 3 (174 from the start codon). Two signals derived from the inherent genome (B6 and CS) and the transgene (MSM/Ms) were detected in the transgenic mice. (**c**) *In situ* hybridization analysis of *Usp46* in the coronal and sagittal sections of the transgenic and nontransgenic mice. (**d**) Transgenic rescue of the shortened immobility time on TST. The behavior on TST was assessed in 339 F_2 mice; however, 49 mice, which climbed on their tails[4], were excluded from the data, and therefore 290 F_2 mice were analyzed. The number of mice used is shown within parentheses. Two-way ANOVA was used to detect the effects of the transgene and congenic genotype. Transgene presence: $F_{1,290} = 55.8$, $P < 9.5 \times 10^{-13}$; congenic genotype: $F_{2,290} = 11.7$, $P < 1.3 \times 10^{-5}$. To confirm whether the transgene increases the TST immobility time in the same congenic genotype, Student's *t*-test was performed ($^{***}P < 0.001$). One-way ANOVA was performed to compare the degree of rescue among the different congenic genotypes; however, no differences were found in any pair of congenic genotypes ($F_{2,144} = 0.63$, $P = 0.53$).

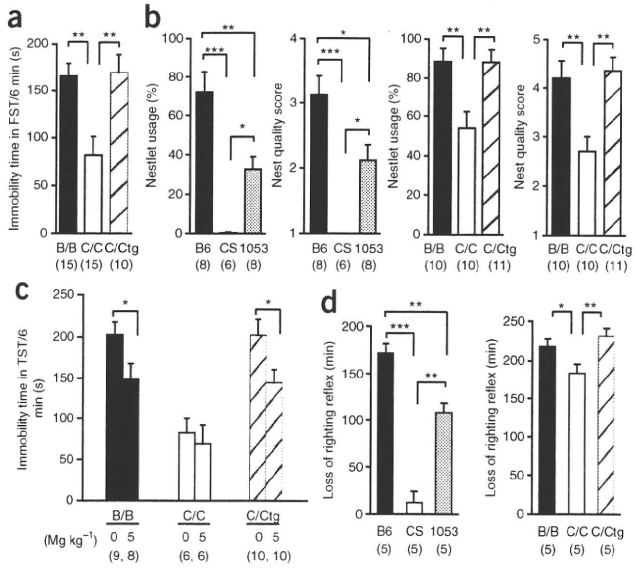

Figure 4 Behavioral pleiotropism of *Usp46* and transgenic rescue. (**a**) Transgenic rescue of the immobility time on FST. The C/C tg strain showed a significantly longer FST immobility time than the C/C strain (one-way ANOVA, $F_{2,37} = 7.1$, $P < 0.0025$). (**b**) The CS and B6.CS-Ngu1053 mice showed a significantly lower nest usage ($F_{2,19} = 19.8$, $P < 2.3 \times 10^{-5}$) and nest quality score ($F_{2,19} = 19.0$, $P < 3.0 \times 10^{-5}$) than the B6 mice. The C/C tg strain showed a significantly higher level of nest usage ($F_{2,28} = 7.2$, $P < 0.0031$) and nest quality score ($F_{2,28} = 8.5$, $P < 0.0013$) than the C/C strain. (**c**) Imipramine administration reduced the immobility time on TST in the B/B and C/C tg strain (B/B, $P < 0.039$; C/C tg, $P < 0.034$), but not in the C/C strain. (**d**) Duration of the loss of righting reflex after administration of muscimol (3 mg kg^{-1}). The CS and B6.CS-Ngu1053 strains showed a significantly shorter duration than the B6 strain (one-way ANOVA, $F_{2,12} = 56.9$, $P < 7.6 \times 10^{-7}$). The transgene increased the duration ($F_{2,14} = 8.5$, $P < 0.0039$). The number of mice used is shown within parentheses. Tukey-Kramer *post hoc* test: $^{***}P < 0.001$, $^{**}P < 0.01$, $^{*}P < 0.05$.

this did not affect the immobility time in the B/B genotype (**Fig. 3d** and **Fig. 4a**; **Supplementary Table 4** online).

Behavioral pleiotropism of *Usp46*

To gain insight into the function of *Usp46*, we subjected the B6.CS-Ngu1053 mice to a number of behavioral tests (open-field, light-dark box, elevated plus-maze, hole-board and nest-building tests). The results of the nest-building and light-dark box tests differed significantly between the B6 and B6.CS-Ngu1053 mice (nestlet usage, $P < 0.01$; nest quality score, $P < 0.05$; time in dark box, $P < 0.02$) (**Fig. 4b**; **Supplementary Fig. 6** online). In the nest-building test, the B6 mice used substantial amounts of nest material and B6.CS-Ngu1053 mice used moderate amounts of nest material, whereas virtually no nest material was used by the CS mice. In the light-dark box test, B6.CS-Ngu1053 mice spent less time in the dark compartment than B6 mice, but the number of times the mice defecated was similar in these strains (defecation, 0.33 ± 0.18 for B6, 0 ± 0 for B6.CS-Ngu1053; $P = 0.11$, Mann-Whitney U test). In addition, we examined the effects of the administration of the antidepressant drug imipramine on the TST immobility time to assess the role of *Usp46* in the antidepressant activity of imipramine. Although imipramine administration significantly reduced immobility time in the B/B strain, no obvious effects were observed in the C/C strain (**Fig. 4c**). The *Usp46* transgene completely rescued the nest-building behavior and the insensitivity to the anti-immobility effects of imipramine (**Fig. 4**).

Involvement of *Usp46* in the regulation of the action of GABA

Because CS mice did not exhibit immobility in the TST and FST, we assumed that the inhibitory action on the behavior might be attenuated. To test this assumption, we first measured the sensitivity to muscimol, a selective $GABA_A$ receptor agonist and a partial agonist for $GABA_C$ receptors, in *Usp46* mutant mice. Because muscimol administration eliminated the righting reflex, we analyzed the duration of loss of the righting reflex. The results revealed that the recovery of the righting reflex was extremely fast in the CS mice ($P < 0.001$ versus B6), and this characteristic was also observed in the B6.CS-Ngu1053 mice ($P < 0.01$ versus B6). The idea that *Usp46* is involved in the attenuated sensitivity to muscimol is supported by the results of the rescue experiment (**Fig. 4d**).

To directly determine whether the *Usp46* mutation indeed altered the $GABA_A$ receptor–mediated inhibitory current, we obtained whole-cell patch-clamp recordings from CA1 pyramidal neurons of the hippocampus, one of the brain regions that strongly expressed *Usp46* as shown by *in situ* hybridization, in slice preparations from the mice with the three genotypes. First, we found no statistical differences in the resting membrane potentials (B/B, –72.7 ± 1.4 mV; C/C, –72.4 ± 1.1 mV; C/C tg, –71.9 ± 1.4 mV) and input resistances (B/B, 134 ± 9.3 MΩ; C/C, 148 ± 9.3 MΩ; C/C tg, 132 ± 8.8 MΩ) of the cells among the three mouse strains. Next, the $GABA_A$ receptor–mediated muscimol currents were recorded by the consecutive application of 0.1, 1.0 and 10.0 μM muscimol. Notably, the muscimol-induced outward current in the cells from the C/C strain was the lowest among all the mice strains at all concentrations examined (**Fig. 5a**). Lastly, we performed miniature inhibitory postsynaptic current (mIPSC) analysis on the same CA1 pyramidal neurons. However, we found no significant differences in the amplitude, rise time, decay time or frequency of the mIPSCs among the three strains of mice (**Fig. 5b**).

Immunohistochemistry

To further study the involvement of *Usp46* in the GABAergic system, we examined the expression of the 67-kDa isoform of glutamic acid

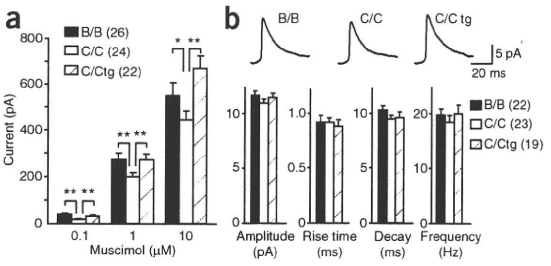

Figure 5 *Usp46* mutation reduces muscimol-induced $GABA_A$ receptor–mediated currents but preserves GABAergic mIPSCs. (**a**) Muscimol-induced currents recorded from CA1 pyramidal neurons. The C/C strain showed a significantly lower amount of muscimol-induced currents than the B/B and C/C tg strains (one-way ANOVA, 0.1 μM: $F_{2,69} = 7.60$, $P < 0.001$; 1 μM: $F_{2,69} = 4.00$, $P < 0.023$; 10 μM: $F_{2,69} = 5.25$, $P = 0.0076$). (**b**) GABAergic mIPSCs in the B/B, C/C and C/C tg strains were not significantly different from each other in amplitude, 20–80% rise time, decay time and frequency. Upper traces are representative mIPSCs of CA1 pyramidal neurons in the three genotypes. Each trace was obtained by averaging the mIPSCs that occurred in a 3-min time window. The number of cells recorded is shown within parentheses (19–26 cells from 4–5 mice; age, 33–41-days-old). Student's *t*-test with Bonferroni correction: $^{**}P < 0.01$, $^{*}P < 0.05$.

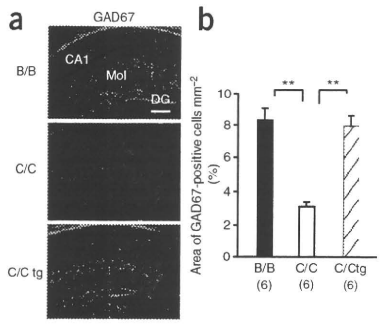

Figure 6 *Usp46* mutation reduces GAD67 immunostaining in the hippocampus. (**a**) Immnostaining against GAD67 in the hippocampus of the B/B, C/C and C/C tg strains. CA1, Cornet d'Ammon 1; DG, dentate gyrus; Mol, molecular layer in the DG; scale bar, 200 μm. (**b**) Quantification of GAD67 expression in the hippocampus of the B/B, C/C and C/C tg strains. The area of GAD67-positive cells mm^{-2} in the hippocampus was significantly decreased in the C/C strain compared with the B/B and C/C tg strains (one-way ANOVA, $F_{2,17} = 23.8$, $P < 2.3 \times 10^{-5}$). $^{**}P < 0.01$.

decarboxylase (GAD67, one of the GABA synthetic enzymes) in the hippocampus by immunohistochemistry[23]. Immunoreactivities against GAD67 were significantly lower (especially in the CA1 region and dentate gyrus in the hippocampus) in the C/C strain relative to the B/B strain, and the immunoreactive phenotype was completely rescued in the C/C tg strain (**Fig. 6**).

DISCUSSION

In the present study, we found that the CS mice showed negligible immobility in the TST and FST. Although in some studies, gender differences in the TST and FST were reported[4,24], both male and female CS mice showed virtually no immobile posture. These characteristics of the TST and FST have not been reported in any inbred mice, even in the genetically modified mice[3]. This unusual characteristic is probably due to a multiple gene system consisting of major (chromosomes 5 and 4) and minor QTLs that act in concert to accelerate the mobility. In fact, a congenic strain with a QTL on chromosome 5 showed intermediate levels in these behavioral tests.

Several groups have already sought to map the QTLs that affect the basal immobility time and the antidepressant response in the TST and FST[7–11]. Notably, two recently reported QTLs that influence the immobility time in the TST overlap with our suggested QTLs on chromosome 4. In particular, one peak position reported previously is very similar to that found in our study[8,10].

Using congenic strains, we narrowed the chromosomal region harboring the quantitative trait gene down to a size of 0.5 Mb. Within this region, 1 EST gene (*1700112M01Rik*) was registered in the Ensembl database. We examined the expression of the EST gene in the brain, but we could not detect any signal by *in situ* hybridization analysis. Sequencing and expression analysis of the other genes located in this critical region led us to the idea that *Usp46* with the 3-bp deletion is the most likely candidate gene. To confirm this, we performed a rescue experiment with transgenic BAC and confirmed that *Usp46* is the quantitative trait gene that affects immobility in the TST and FST. *Usp46*, which encodes a deubiquitinating enzyme, is implicated in the ubiquitin-proteasome system, which is critical for the regulation of many cellular processes. In this system, the pathway involving protein ubiquitination and proteasomal degradation has been the focus of many studies. However, the removal of ubiquitin, which is mediated by deubiquitinating enzymes, has not been well studied[25,26]; thus, little is known regarding the physiological functions of USP46. The present study demonstrates for the first time (to our knowledge) that USP46 functions to regulate several behavioral processes, including basal immobility, the anti-immobility effects of imipramine, nest building and the muscimol-induced righting reflex.

To gain insight into the functions of this enzyme, it should be noted that the muscimol-induced righting reflex is affected by the mutation in *Usp46* and is rescued by the transgene. This result suggests that *Usp46* is involved in the regulation of GABA action. The involvement of *Usp46* in GABAergic mechanisms is supported by results showing that the immobility time in the TST and FST is reduced in mice that lack GABA transporter subtype 1 (GAT1)[27], and by results showing that nesting behavior is impaired in mice deficient in the gene encoding $GABA_A$ receptor subunit β3 (*Gabrb3*)[28] and in mice deficient in the gene encoding $GABA_A$ receptor subunit δ (*Gabrd*)[29]. It is reported that imipramine has similar effects for reducing the immobility time in both the GAT1-knockout mice and the wild-type mice[27]; this result is different from our result that normal *Usp46* is required for anti-immobility effects. Our results suggest that *Usp46* may affect GABAergic systems by mechanisms other than those involving GAT1. It is notable that while mapping QTLs, other investigators[8] also focused on the genes coding for the $GABA_A$ receptor subunits as candidates affecting the immobility time in the TST and FST.

To further understand the involvement of *Usp46* in the GABAergic system, we performed electrophysiological analysis of the hippocampal CA1 pyramidal neurons. No significant changes were observed among the three genotypes (B/B, C/C and C/C tg) in the basic cellular electrophysiological properties such as resting membrane potentials and input resistances; however, we found that the muscimol-induced outward current mediated by $GABA_A$ receptors is significantly (35% at the maximum) decreased in the C/C strain compared with the B/B and C/C tg strains. This finding suggested that the *Usp46* transgene might have rescued the GABAergic responses, thereby normalizing behavioral abnormalities as observed in the C/C tg strain. However, it is unlikely that the $GABA_A$ receptor *per se* is qualitatively altered in the C/C strain, because no differences were found among the three strains with regard to the physiological properties of the $GABA_A$ receptor channel current (such as the amplitude, rise time and decay time). The frequency of mIPSCs depends on the number of synapses and the probability of neurotransmitter release from presynaptic membranes[30], but there were no significant differences in the frequency of mIPSCs among the three strains. Alternatively, it could be argued that changes in the number of extrasynaptic $GABA_A$ receptors cause diminished muscimol-induced current responses in the C/C strain[31].

The involvement of *Usp46* in the GABAergic system is further supported by a marked reduction in GAD67 expression, as determined by immunohistochemistry. Because GAD67 catalyzes the decarboxylation of glutamate to GABA, *Usp46* seems to be involved in GABA synthesis. However, unlike in the GABA-producing neurons, the electrophysiological changes were observed in the hippocampal CA1 pyramidal neurons, which are excitatory neurons. Thus, it is likely that *Usp46* mutation extensively affects the GABAergic system. The pre- and postsynaptic changes observed in these experiments might be explained by the developmental defects caused by a reduction in the levels of GABA, which acts as a neurotrophic factor. It is known that GABA affects several developmental processes of the nervous system, such as proliferation, migration, differentiation, synaptic maturation and cell death[23,32,33]. These changes might lead to the diminished responses to muscimol in the *Usp46* mutant mice. Another interpretation might be that *Usp46* regulates different protein substrates, which independently affect the pre- and postsynaptic

events. In any case, further investigation is clearly needed to determine how the *Usp46* transgene affects the GABAergic system.

In summary, we identified *Usp46* as a quantitative trait gene responsible for the immobility in the TST and FST. Because *Usp46* appears to be implicated in a wide range of behavioral functions regulated by the GABAergic system, the present results might contribute to the understanding of the neural and genetic mechanisms that underlie the mental disorders associated with this gene.

METHODS

Animals. We purchased the C57BL/6J (B6) mice from CLEA Japan Inc., and CS mice were originally provided by T. Namikawa (Nagoya University). The mice were housed under a 12-h light and dark cycle (LD 12:12, 7:00 on, 19:00 off) with free access to food and water in our animal facility at a temperature maintained at approximately 24 °C. We performed TST and FST on both male and female mice aged 8–12 weeks. The other tests were conducted only on male mice aged 9–24 weeks.

For all the experiments, the animals were treated in accordance with the guidelines issued by Nagoya University, Faculty of Pharmaceutical Sciences of Meijo University and Tokyo Metropolitan Institute of Gerontology.

QTL analysis. Initially, we performed interval mapping using a least-squares regression method (Map Manager QTXb20) on 203 F_2 hybrids (105 male, 98 female) produced by intercrossing F_1 mice obtained from B6 and CS mice using 56 Mit markers (2 to 3 markers per chromosome) purchased from Research Genetics Inc. When significant QTLs were detected, we conducted further analysis using additional markers ($n = 69$) for flanking potential QTLs (**Supplementary Table 5** online). The likelihood of odds (LOD) scores at genome-wide significance (5%) and suggestive (63%) levels were determined by 1,000 runs of a permutation test[34]. The LOD scores at the genome-wide significance (5%) and suggestive (63%) levels for TST and FST were 3.30 and 1.95, respectively. To confirm the presence of the main-effect QTLs detected using Map Manager QTXb20, we performed nonparametric interval mapping using the computer package R/qtl version 1.08-56 (ref. 35), because of the extreme skew in the distribution of both traits (**Fig. 1a**). Epistatic interaction analysis was performed using Map Manager QTXb20, as described previously[36]. The significance of the overall effect was examined by 1,000 runs of a permutation test using Map Manager QTXb20.

Congenic strains. Congenic strains were developed by continually backcrossing (at least six times) a donor strain that harbors the genomic region of interest with B6 by a marker-assisted breeding strategy[37]. We used Mit SSLP markers (**Supplementary Table 5**); however, if no known polymorphic markers existed, we identified long di- or trinucleotide repeats in the genomic sequence and designed primers to amplify these regions. These markers were named *D5B6CS* (**Supplementary Table 6** online). We developed 17 congenic or subcongenic strains on a B6 genetic background that contained various chromosome 5 regions of the CS mice from the Mit marker *D5Mit300* (51.8 Mb) to *D5Mit259* (89.70 Mb) (**Supplementary Fig. 2**). We named these strains B6.CS-Ngu and so on based on the Mouse Genome Informatics guidelines for nomenclature of mouse strains.

Candidate gene analysis. The sequence of each gene in the B6 mice was obtained from Mouse Genome Informatics (http://www.informatics.jax.org/), and primers were designed to amplify the full-length open reading frame (ORF). We carried out sequencing analysis to detect mutations in CS and B6.CS-Ngu1053 in comparison with B6. Total RNA was extracted from the whole brain using TRIzol reagents (Invitrogen). Superscript III reverse transcriptase (Invitrogen) and total RNA with oligo(dT) were used for first-strand complementary DNA synthesis, and candidate genes containing the full-length ORF were amplified by PCR and directly sequenced using the Big Dye cycle sequencing kit (Applied Biosystems) on an ABI 3130 automated sequencer. Because *2700023E23Rik* showed a very low expression level in the brain, we amplified the putative ORF from the genomic DNA. The primers obtained by the amplification of the ORF are listed in **Supplementary Table 7** online.

We carried out *in situ* hybridization to compare the mRNA expression levels among the B6, CS and B6.CS-Ngu1053 strains. We killed the animals by decapitation, and we immediately removed the brains to avoid acute changes in gene expression. *In situ* hybridization was carried out as described previously[38]. Antisense 45-nucleotide oligonucleotide probes were labeled with [^{33}P]dATP (NEN) using terminal deoxyribonucleotidyl transferase (Gibco BRL). Hybridization was carried out overnight at 42 °C. After the glass slides were washed, they were air-dried and apposed to a Biomax-MR film (Eastman Kodak Co.) for 2 weeks with ^{14}C standards (American Radiolabeled Chemicals). The relative optical densities were measured using a computed image-analyzing system (Image Gauge) and were converted into the respective relative radioactive values (nCi) by ^{14}C standards. Specific hybridization signals were obtained by subtracting the background values obtained from the adjacent brain areas that did not exhibit hybridization signals. The oligonucleotide probes are listed in **Supplementary Table 7**.

Transgenic strain. To obtain the transgenic mice for the behavioral tests, we first generated the B6 founder mice having the *Usp46* transgene. These mice were crossed with mice homozygous (C/C) or heterozygous (B/C) for the allele at the congenic region of the B6.CS-Ngu1053 strain. The heterozygous mice with the *Usp46* transgene obtained by this cross were then crossed with B6.CS-Ngu1053 heterozygous mice, producing six different genetic constitutions in the progeny (**Fig. 3a**).

The mouse BAC clone (*MSMG01-414M7*, 74.31–74.48 Mb) originating from the MSM/Ms strain covering the *Usp46* locus (including 12,163 bp upstream and 81,996 bp downstream from the 5′ and 3′ ends) was obtained from RIKEN BioResource Center. We cloned genomic DNA into the pBACe3.6 vector at the EcoRI and EcoRI methylase cloning sites[39]. We obtained BAC DNA from 500 ml of LB using 12.5 μg ml^{-1} chloramphenicol and a NucleoBond BAC 100 kit (MACHEREY-NAGEL) according to the supplier's instructions. To separate the 162-kb MSM/Ms-derived DNA from the vector sequence, the circular BAC clone was digested with NotI (Takara), and the restriction fragments were separated using pulsed-field gel electrophoresis (PFGE) for 18 h on 1% pulse field certified agarose (BioRad) gel under the following conditions: included angle, 120°; 6 V cm^{-1}; and switch-time ramping from 0.1 s to 12 s (CHEF Mapper II, BioRad). After the PFGE run, the marker lanes on either side of the preparative lane and up to ~5 mm were cut off and stained with ethidium bromide. The position of the BAC band was marked with a sterile razor blade, and the part of the preparative lane containing the BAC DNA was excised. The excised gel slice was dialyzed in TE buffer.

The isolated BAC DNA was injected at a concentration of 1 ng μl^{-1} into fertilized mouse oocytes isolated from B6 mating. Oocytes that survived injection were transferred later on the same day to both oviducts of pseudo-pregnant ICR foster mothers. Transgenic mice were identified by both PCR and Southern blot analysis of genomic DNA prepared from the tail. The sets of primers used to identify the transgenic animals are listed in **Supplementary Table 8** online. For transgene analysis, 10 μg of genomic DNA were digested with BamHI and size fractionated on a 1% agarose gel in 1× TAE. The Southern blots were hybridized with [^{32}P]-labeled genomic probes (570 bp) containing *MSMG01-414M07* sequences.

TST and FST. After weaning, mice of the same sex were maintained in a group (1–5 mice per cage) under an LD 12:12 cycle (7:00 on, 19:00 off) at approximately 24 °C with food and water *ad libitum* in our animal facility. Before the TST and FST, these mice were moved to the animal room adjacent to the test room where their behaviors were assayed, and the mice were kept there for 1 week under the same conditions as those before moving. We assayed mice aged 8–12 weeks during the light (11:00–16:00) after at least a 2-h adaptation to the test room. The procedure for TST was based on a previous study[2], but with slight modifications[40]. In our test, the mice were suspended by their tails using an elastic band (5 cm in diameter) attached to the tail by adhesive tape (approximately 1 cm from the tip of the tail), and the elastic band was hooked on a horizontal rod. The distance between the tip of the nose of the mouse and the floor was approximately 20 cm. The mice were suspended for a period of 7 min, and the time spent immobile during the last 6 min of 7 min was scored for each individual by an observer blinded to the genotype.

On day 2 after the TST, the pre-session of the FST was performed. We placed the mice in plastic cylinders (height, 30 cm; diameter, 20 cm) containing water (25 ± 1 °C; depth, 15 cm) for 15 min. On the next day, we placed the mice in the same cylinder and scored the time immobile during the last 6 min of the 7 min of forced swimming[22,41].

In the TST, we examined the effects of administration of imipramine (Wako) on the immobility time. The mice were intraperitoneally injected with 10 ml kg^{-1} of the vehicle (saline) or imipramine (5 mg kg^{-1}) and subjected to the TST at 40 min after injection.

Muscimol-induced righting reflex. Mice were subcutaneously injected with muscimol (Bachem, 3 mg kg^{-1}) dissolved in saline and placed on their backs into a V-shaped trough every 10 min after the injection to measure the latency until the return of the righting reflex. The loss of the righting reflex was defined as the inability of the mouse to right itself within 30 s. The recovery of the righting reflex was determined when a mouse righted twice in the 2 consecutive 30-s trials.

Nest building. Approximately 1 h before the dark phase of LD 12:12, we placed the mice individually in a cage with wood-chip bedding and one nestlet made of pressed cotton (Lillico; 2.5 g, 5 cm × 5 cm). Based on a previous report[42], the nests were assessed on the next morning using the following rating scale: 1, >90% intact; 2, 50–90% intact; 3, 10–50% intact; 4, 0–10% intact, but flat nest; 5, 0–10% intact, with walls higher than the height of the mouse. The amount of nest material was measured by subtracting the weight of the untorn nestlet pieces (loose material and bedding were brushed off) from the total weight.

Open-field test. Each mouse was placed in the center of a gray plastic box (40 × 40 × 40 cm) with the floor divided into 64 compartments (5 × 5 cm each) and was allowed to freely explore for 5 min under 40-lx to 50-lx fluorescent light. The test was conducted during the light phase of LD 12:12 (11:00–16:00). During the test, the number of boundaries of the compartment passed, grooming, rearing and defecation were scored.

Light-dark box test. The light-dark box consisted of a dark and a light compartment (each compartment: width, 15 cm; height, 15 cm; length, 25 cm) that were divided by a partition with a small opening (width, 42 mm; height, 44 mm) through which the mice could move between the compartments. The dark and light compartments were made of black and clear plexiglas, respectively. During the light phase of LD 12:12 (11:00–16:00), each mouse was placed in the center of the light compartment and allowed to freely explore the box for 5 min under 40-lx to 50-lx fluorescent light. The inside of the dark compartment was not illuminated. The observer scored the number of light-dark transitions between the two compartments, the total time spent in the dark compartment and the number of episodes of defecation[41].

Elevated plus-maze test. The elevated plus-maze consists of two open arms (width, 8 cm; length, 25 cm) and two closed arms (width, 8 cm; height, 20 cm; length, 25 cm) that extend from a common central platform (8 × 8 cm)[41,43]. This apparatus was elevated to a height of 50 cm above the floor. Each mouse was placed on the center square, facing an open arm, and was allowed to freely explore for 5 min under 40-lx to 50-lx fluorescent light. We scored the number of open and closed arm entries, the total time spent on the open arm and the number of episodes of defecation. We conducted this test during the light phase of LD 12:12 (11:00–16:00).

Y-maze test. We examined short-term memory by the Y-maze test based on the method reported previously[22]. The Y-maze was made of wood that had been painted black, and each arm was 40 cm long, 12 cm high, 3 cm wide at the bottom and 10 cm wide at the top. The arms converged at a central equilateral triangular area with its longest axis measuring 4 cm. The apparatus was placed on the floor of the experimental room and was illuminated with a 100 W bulb placed 200 cm above. Each mouse was placed at the end of one arm and allowed to move freely through the maze during an 8-min session, and the series of arm entries was recorded visually. The alternation behavior was defined by successive entries into the three arms, on overlapping triplet sets, and such behavior (%) was expressed as the ratio of actual alternations (defined as the total number of arm entries minus two), multiplied by 100. After the experiments, we counted the number of arm entries.

Prepulse inhibition test. The apparatus used and the procedure were the same as reported previously[44]. The startle chambers (SR-LAB; San Diego Instruments) consisted of nonrestrictive plexiglas cylinders, 3.8 cm in diameter and 13 cm long, resting on a plexiglas platform in a ventilated and well-lit chamber connected with a measurement cage containing a signal amplification sensor. A high-frequency speaker mounted 33 cm above the cylinder produced all acoustic stimuli. A piezoelectric accelerometer was mounted under each cylinder and detected transduced animal movements. A computer and interface assembly digitized and stored the data. A dynamic calibration system (SR-LAB; San Diego Instruments) was used to ensure comparable sensitivities across the chambers. The sound levels were measured in decibels. The background white noise was 70 dB in the soundproof box of the loudspeaker as measured from the upper part of the measurement cage.

Six different trial types were presented in the test session: 40-ms broadband 87-dB (prepulse-alone trial) and 118-dB (pulse-alone trial) bursts; three different prepulse (pp) + pulse (p) trials in which 40-ms-long 10-dB (pp10p118), 13-dB (pp13p118) or 17-dB (pp17p118) stimuli above a 70-dB background white noise preceded the 118-dB pulse by 100 ms (onset to onset); and a no-stimulus trial, in which only the background white noise was presented[44]. Thus, the six trial types presented were pulse alone, prepulse alone, pp10p118, pp13p118, pp17p118 and no stimulus. Each of the six different trial types was presented in a random order eight times. The intertrial interval was 30 s. The test session consisted of 48 trials. The session began with a 5-min acclimatization period followed by test session. The vibration was examined 100 ms after auditory stimulation (pulse) as the startle amplitude. The prepulse inhibition was obtained as follows: prepulse inhibition = ((pulse-alone response × (prepulse + pulse response))/(pulse-alone response)) × 100.

Hole board test. The hole board test consisted of a 40-cm square plane with 16 flush-mounted cylindrical holes (each measuring 3 cm in diameter) distributed 4 × 4 in an equidistant, grid-like manner[45]. The mice were placed one by one at the center of the board and were allowed to move about freely for a period of 5 min each under 40 lx to 50 lx. During the test (the light phase of LD 12:12, 11:00–16:00), the number of head dips (defined as placing the head into a hole) was counted.

Electrophysiology. Hippocampal slices (250 μm thick) were obtained from the B/B, C/C and C/C tg strain aged P33–P41 as described previously[46]. Whole-cell patch-clamp recordings were performed from hippocampal CA1 pyramidal neurons using an EPC9/2 amplifier (HEKA Electronik) and a PowerLab (ADI Instruments) with infrared-differential interference contrast visualization. Patch pipettes (3–5 MΩ) were filled with a solution containing (in mM) 124 Cs-methanesulfonate, 11 KCl, 2 $MgCl_2$, 0.1 EGTA, 10 HEPES, 4 Na_2-ATP, 0.3 GTP, 5 QX-314 and 0.5% biocytin (brought to pH 7.3 with CsOH, osmolarity 280 mOsm). The liquid junction potential of the solution was 9.65 mV and corrected. $GABA_A$ receptor–mediated current was recorded as an outward current at a holding potential of 0 mV in the presence of the NMDA receptor antagonist D-(−)-2-amino-5-phosphonopentanoic acid (AP5; 25 μM), the AMPA receptor antagonist 6-cyano-7-nitroquinoxaline-2,3-dione (CNQX; 10 μM) and tetrodotoxin (TTX; 0.5 μM). Muscimol was bath-applied for 2.5 min to the same cells recorded at increasing concentrations of 0.1, 1.0 and 10.0 μM, and the maximum current at each concentration was measured as the muscimol current at each concentration. Miniature inhibitory synaptic currents (mIPSCs) were analyzed offline with MiniAnalysis 6.0.7 (Synaptosoft). The detection threshold of miniature currents was set at twice the baseline noise.

Immunohistochemistry. Immunohistochemistry was performed as previously described[47] with minor modifications. We fixed brains with 4% paraformaldehyde in phosphate-buffered saline (PBS) and obtained hippocampal slices (20-μm thick) with a cryostat (MICROM HM560; MICRO EDGE) according to a previously described atlas[48]. Fluorescent images were captured directly in some samples, and images were acquired with a confocal microscope (LSM510; Carl Zeiss) or a light microscope (AxioCam HRc; Carl Zeiss). Monoclonal mouse anti-GAD67 (1:100, Millipore Corporation) diluted in PBS containing 0.01% Triton X-100 and 5% rabbit serum was applied to sections, which were then incubated overnight at 4 °C. After washing by 0.01% Triton X-100 in PBS, rabbit anti-mouse Alexa Fluor 488 (1:1000, Invitrogen) was added to sections as a fluorescently conjugated secondary antibody for 2 h at room temperature (approximately 20 °C). Every fourth, fifth and sixth section throughout the hippocampus (total 12 sections) was processed for GAD67 immnohistochemistry. To quantify the immunoreactivities of GAD67, we used the imaging software WinRoof (Mitani Co. Ltd.)[47,49]. The areas of GAD67-positive cells mm^{-2} were measured in the hippocampus. The average of the three determinations for each mouse was used for statistical analysis.

Statistics. The results are represented as the mean ± s.e.m. One-way ANOVA using a Tukey-Kramer *post hoc* test, Student's *t*-test with Bonferroni correction or two-way ANOVA was used for comparison among multiple datasets; Student's *t*-test or Mann-Whitney *U* test was used for comparison between two groups.

Note: Supplementary information is available on the Nature Genetics website.

ACKNOWLEDGMENTS

We thank the late M. Ukai (Meijo University) for his helpful suggestions and for providing the facilities for the behavioral experiments, A. Yoshiki (RIKEN BRC) for his useful suggestions regarding the rescue experiment with transgenic mice, S. Yasuo (Johann Wolfgang Goethe-University Frankfurt) for her guidance on the *in situ* hybridization experiment, RIKEN BRC for providing the mice and the Nagoya University Radio-isotope Center for allowing us to use their facilities. This research was supported in part by a Grant-in-Aid for Scientific Research to S.E. and by the Academic Frontier Project for Private Universities (2007–2011) from the Ministry of Education, Culture, Sports, Science and Technology of Japan to T.M and T.N.

AUTHOR CONTRIBUTIONS

S.E. designed the experiments, supervised the project and prepared the manuscript. S.T. designed and performed most of the experiments, analyzed the data and prepared the manuscript. H.S. performed the behavioral tests. T.M. and T.K. supervised the behavioral experiments. T.N. organized GABA-related experiments, and M.Mi, T.A. and M.Ma. performed electrophysiological experiments. M.N. contributed to histological examination. J.K., S.I. and A.I. conducted the QTL analysis. K.A. supervised the production of BAC transgenic mice. Y.I. and S.I. contributed to congenic strain breeding and phenotyping. T.Y. provided the facilities and provided technical support.

Published online at http://www.nature.com/naturegenetics/
Reprints and permissions information is available online at http://npg.nature.com/reprintsandpermissions/

1. Porsolt, R.D., Lepichon, M. & Jalfre, M. Depression—new animal-model sensitive to antidepressant treatments. *Nature* **266**, 730–732 (1977).
2. Steru, L., Chermat, R., Thierry, B. & Simon, P. The tail suspension test—a new method for screening antidepressants in mice. *Psychopharmacology (Berl.)* **85**, 367–370 (1985).
3. Cryan, J.F. & Mombereau, C. In search of a depressed mouse: utility of models for studying depression-related behavior in genetically modified mice. *Mol. Psychiatry* **9**, 326–357 (2004).
4. Cryan, J.F., Mombereau, C. & Vassout, A. The tail suspension test as a model for assessing antidepressant activity: review of pharmacological and genetic studies in mice. *Neurosci. Biobehav. Rev.* **29**, 571–625 (2005).
5. Watanabe, A. *et al.* Fabp7 maps to a quantitative trait locus for a schizophrenia endophenotype. *PLoS Biol.* **5**, e297 (2007).
6. Flint, J., Valdar, W., Shifman, S. & Mott, R. Strategies for mapping and cloning quantitative trait genes in rodents. *Nat. Rev. Genet.* **6**, 271–286 (2005).
7. Turri, M.G., Datta, S.R., DeFries, J., Henderson, N.D. & Flint, J. QTL analysis identifies multiple behavioral dimensions in ethological tests of anxiety in laboratory mice. *Curr. Biol.* **11**, 725–734 (2001).
8. Yoshikawa, T., Watanabe, A., Ishitsuka, Y., Nakaya, A. & Nakatani, N. Identification of multiple genetic loci linked to the propensity for "behavioral despair" in mice. *Genome Res.* **12**, 357–366 (2002).
9. Crowley, J.J., Brodkin, E.S., Blendy, J.A., Berrettini, W.H. & Lucki, I. Pharmacogenomic evaluation of the antidepressant citalopram in the mouse tail suspension test. *Neuropsychopharmacology* **31**, 2433–2442 (2006).
10. Liu, X., Stancliffe, D., Lee, S., Mathur, S. & Gershenfeld, H.K. Genetic dissection of the tail suspension test: a mouse model of stress vulnerability and antidepressant response. *Biol. Psychiatry* **62**, 81–91 (2007).
11. Lad, H.V., Liu, L., Paya-Cano, J.L., Fernandes, C. & Schalkwyk, L.C. Quantitative traits for the tail suspension test: automation, optimization, and BXD RI mapping. *Mamm. Genome* **18**, 482–491 (2007).
12. Suzuki, T. *et al.* Quantitative trait locus analysis of abnormal circadian period in CS mice. *Mamm. Genome* **12**, 272–277 (2001).
13. Abe, H., Honma, S., Honma, K., Suzuki, T. & Ebihara, S. Functional diversities of two activity components of circadian rhythm in genetical splitting mice (CS strain). *J. Comp. Physiol. [A]* **184**, 243–251 (1999).
14. Abe, H., Honma, S. & Honma, K. Daily restricted feeding resets the circadian clock in the suprachiasmatic nucleus of CS mice. *Am. J. Physiol. Regul. Integr. Comp. Physiol.* **292**, R607–R615 (2007).
15. Ebihara, S., Miyazaki, S., Sakamaki, H. & Yoshimura, T. Sleep properties of CS mice with spontaneous rhythm splitting in constant darkness. *Brain Res.* **980**, 121–127 (2003).
16. Belknap, J.K. *et al.* QTL analysis and genomewide mutagenesis in mice: complementary genetic approaches to the dissection of complex traits. *Behav. Genet.* **31**, 5–15 (2001).
17. Flint, J. & Mott, R. Finding the molecular basis of quantitative traits: successes and pitfalls. *Nat. Rev. Genet.* **2**, 437–445 (2001).
18. Crawley, J.N. Behavioral phenotyping of transgenic and knockout mice: experimental design and evaluation of general health, sensory functions, motor abilities, and specific behavioral tests. *Brain Res.* **835**, 18–26 (1999).
19. Bourin, M. & Hascoet, M. The mouse light/dark box test. *Eur. J. Pharmacol.* **463**, 55–65 (2003).
20. Karl, T., Pabst, R. & von Horsten, S. Behavioral phenotyping of mice in pharmacological and toxicological research. *Exp. Toxicol. Pathol.* **55**, 69–83 (2003).
21. Braff, D.L., Geyer, M.A. & Swerdlow, N.R. Human studies of prepulse inhibition of startle: normal subjects, patient groups, and pharmacological studies. *Psychopharmacology (Berl.)* **156**, 234–258 (2001).
22. Mamiya, T. *et al.* Effects of pre-germinated brown rice on beta-amyloid protein-induced learning and memory deficits in mice. *Biol. Pharm. Bull.* **27**, 1041–1045 (2004).
23. Chattopadhyaya, B. *et al.* GAD67-mediated GABA synthesis and signaling regulate inhibitory synaptic innervation in the visual cortex. *Neuron* **54**, 889–903 (2007).
24. Solberg, L.C. *et al.* Sex- and lineage-specific inheritance of depression-like behavior in the rat. *Mamm. Genome* **15**, 648–662 (2004).
25. Amerik, A.Y. & Hochstrasser, M. Mechanism and function of deubiquitinating enzymes. *Biochim. Biophys. Acta* **1695**, 189–207 (2004).
26. Nijman, S.M. *et al.* A genomic and functional inventory of deubiquitinating enzymes. *Cell* **123**, 773–786 (2005).
27. Liu, G.X. *et al.* Reduced anxiety and depression-like behaviors in mice lacking GABA transporter subtype 1. *Neuropsychopharmacology* **32**, 1531–1539 (2007).
28. DeLorey, T.M., Sahbaie, P., Hashemi, E., Homanics, G.E. & Clark, J.D. Gabrb3 gene deficient mice exhibit impaired social and exploratory behaviors, deficits in non-selective attention and hypoplasia of cerebellar vermal lobules: a potential model of autism spectrum disorder. *Behav. Brain Res.* **187**, 207–220 (2008).
29. Maguire, J. & Mody, I. GABA(A)R plasticity during pregnancy: relevance to postpartum depression. *Neuron* **59**, 207–213 (2008).
30. Korn, H. & Faber, D.S. Quantal analysis and synaptic efficacy in the CNS. *Trends Neurosci.* **14**, 439–445 (1991).
31. Liang, J. *et al.* Mechanisms of reversible GABAA receptor plasticity after ethanol intoxication. *J. Neurosci.* **27**, 12367–12377 (2007).
32. Meier, E., Belhage, E., Drejer, J. & Schousboe, A. The expression of GABA receptors on cultured cerebellar granule cells is influenced by GABA. in *Neurotrophic Activity of GABA During Development* (eds. Redburn, D.A. & Shousboe, A.) 139–159 (Alan R. Liss, Inc., New York,, 1987).
33. Owens, D.F. & Kriegstein, A.R. Is there more to GABA than synaptic inhibition? *Nat. Rev. Neurosci.* **3**, 715–727 (2002).
34. Churchill, G.A. & Doerge, R.W. Empirical threshold values for quantitative trait mapping. *Genetics* **138**, 963–971 (1994).
35. Broman, K.W., Wu, H., Sen, S. & Churchill, G.A. R/qtl: QTL mapping in experimental crosses. *Bioinformatics* **19**, 889–890 (2003).
36. Ishikawa, A., Hatada, S., Nagamine, Y. & Namikawa, T. Further mapping of quantitative trait loci for postnatal growth in an inter-sub-specific backcross of wild *Mus musculus* castaneus and C57BL/6J mice. *Genet. Res.* **85**, 127–137 (2005).
37. Markel, P. *et al.* Theoretical and empirical issues for marker-assisted breeding of congenic mouse strains. *Nat. Genet.* **17**, 280–284 (1997).
38. Yoshimura, T. *et al.* Molecular analysis of avian circadian clock genes. *Brain Res. Mol. Brain Res.* **78**, 207–215 (2000).
39. Abe, K. *et al.* Contribution of Asian mouse subspecies *Mus musculus* molossinus to genomic constitution of strain C57BL/6J, as defined by BAC-end sequence-SNP analysis. *Genome Res.* **14**, 2439–2447 (2004).
40. Ukai, M., Maeda, H., Nanya, Y., Kameyama, T. & Matsuno, K. Beneficial effects of acute and repeated administrations of sigma receptor agonists on behavioral despair in mice exposed to tail suspension. *Pharmacol. Biochem. Behav.* **61**, 247–252 (1998).
41. Miyamoto, Y. *et al.* Lower sensitivity to stress and altered monoaminergic neuronal function in mice lacking the NMDA receptor epsilon 4 subunit. *J. Neurosci.* **22**, 2335–2342 (2002).
42. Deacon, R.M. Assessing nest building in mice. *Nat. Protoc.* **1**, 1117–1119 (2006).
43. Mamiya, T., Noda, Y., Nishi, M., Takeshima, H. & Nabeshima, T. Enhancement of spatial attention in nociceptin/orphanin FQ receptor-knockout mice. *Brain Res.* **783**, 236–240 (1998).
44. Ukai, M., Okuda, A. & Mamiya, T. Effects of anticholinergic drugs selective for muscarinic receptor subtypes on prepulse inhibition in mice. *Eur. J. Pharmacol.* **492**, 183–187 (2004).
45. Ghelardini, C. *et al.* Antisense knockdown of the Shaker-like Kv1.1 gene abolishes the central stimulatory effects of amphetamines in mice and rats. *Neuropsychopharmacology* **28**, 1096–1105 (2003).
46. Miura, M., Saino-Saito, S., Masuda, M., Kobayashi, K. & Aosaki, T. Compartment-specific modulation of GABAergic synaptic transmission by mu-opioid receptor in the mouse striatum with green fluorescent protein-expressing dopamine islands. *J. Neurosci.* **27**, 9721–9728 (2007).
47. Niwa, M. *et al.* A novel molecule "shati" is involved in methamphetamine-induced hyperlocomotion, sensitization, and conditioned place preference. *J. Neurosci.* **27**, 7604–7615 (2007).
48. Franklin, K.B.J. & Paxinos, G. *The Mouse Brain: in Stereotaxic Coordinates* (Academic Press, San Diego, 1997).
49. Kuwahara, M., Sugimoto, M., Tsuji, S., Miyata, S. & Yoshioka, A. Cytosolic calcium changes in a process of platelet adhesion and cohesion on a von Willebrand factor-coated surface under flow conditions. *Blood* **94**, 1149–1155 (1999).

特集◤喫煙をめぐる諸問題◢

禁煙補助薬の効果②
—バレニクリンによる治療法—

Smoking cessation therapy with varenicline

名城大学大学院薬学研究科薬品作用学教室 **Tursun Alkam**
名城大学大学院薬学研究科薬品作用学教室教授／
名城大学比較認知科学研究所所長／
NPO J-DO 医薬品適正使用推進機構理事長 **鍋島 俊隆** *Toshitaka Nabeshima*

Key words
喫煙，ニコチン，依存症，バレニクリン，禁煙

Summary

日本の約50%の男性と20%の女性は喫煙している。喫煙は，人体各臓器に影響を及ぼし，健康全般を阻害する。喫煙者は，タバコによる悪影響を認識していても，依存症に侵されているので禁煙できない。タバコ依存症はニコチンにより誘発されると考えられる。ニコチンは，ニコチンアセチルコリン受容体(nAChRs)の$\alpha4\beta2$サブユニットを刺激し，依存症を誘発する。$\alpha4\beta2$ nAChRsの部分アゴニストとして，禁煙治療薬バレニクリンがFDAによって2006年に承認されている。これまで日本国内外で行われた禁煙薬臨床試験結果から，バレニクリンは禁煙の第１選択薬として推奨されている。本稿は最近の知見をふまえ，ニコチンによる依存症の形成機序およびバレニクリンによる禁煙治療の根拠に関して概説する。

喫煙者のほとんどは喫煙を有害なものとして認識しており，節煙または禁煙したいと思っている。しかし残念なことに，禁煙を試みた人々のうち，ほとんど１ヵ月以内に生じる渇望により約85%以上は禁煙できず，６ヵ月間では３%しか禁煙できない[1]。喫煙者はニコチンに依存しているため休みなく喫煙する。依存症は，タバコに含まれるニコチンに継続的に長期に脳が曝され，脳の機能が変化することによって誘導される。ニコチンは，報酬効果(急性の満足感，快感)を惹起し，渇望(さらに吸いたいという欲望)をコントロールしている報酬経路を活性化するため，依存症を引き起こす。喫煙すると，血流によってニコチンは急速に脳に運ばれ，10秒以内にニコチンレベルはピークに達し，喫煙者は心地よい気持ちになる。しかし，ニコチンの報酬効果(快感)は速やかに消失するため，喫煙者はニコチンの快い効果を維持し，過敏性・うつ状態・あるいは不安といった禁断症状を防ぐために喫煙を続ける。

ニコチンは，報酬経路の中心皮質辺縁(MCL)ドーパミン(DA)作動性神経系においてDAの遊離を促進する。DAが遊離されると心地よい気持ちになるので，ニコチンに対して容易に依存が形成される[2]。MCLDA作動性神経系は，ニコチンの報酬効果の発現に重要な役割および基本的な役割を果た

す。MCLDA作動性神経系は，中脳の腹側被蓋野(VTA)のDAニューロンから始まり，側坐核(NAc)，扁桃体，および前頭前皮質へと投射されている[3]。VTAでのDAニューロンの活性は，主に前頭前皮質からの興奮性のグルタミン酸作動性入力，脳幹の核からのコリン作動性入力，およびVTA内またはNAcからの抑制性γ-アミノ酪酸(GABA)作動性入力によって調節されている。ニコチンを自己投与するとNAc中のDAレベルは上昇し，さらにこのDAの上昇によって快感が得られるため，依存の獲得段階に際してニコチン自己投与がさらに増える[4]。逆に，NAcにおけるDA終末を化学的に損傷するとニコチンの自己投与が減少する[5][6]。

ニコチンは，ニコチン性アセチルコリン受容体(nAChRs)に結合して活性化する。nAChRsは，シナプス前終末，軸索，細胞体樹状突起，あるいはシナプス後細胞に局在している。脳のnAChRsは，カルシウムに対して高い透過性をもつホモメリック五量体イオンチャネルまたはヘテロメリック五量体イオンチャネルであり，9つのα-サブユニット(α2～10)および3つのβ-サブユニット(β2～4)から構成されている[7][8]。脳内には，α4β2-含有ヘテロマーと，やや少ないがα7-含有ホモマーの2種類のnAChRsが分布しており[9][10]，ニコチンで刺激すると，DA，グルタミン酸，またはGABAのような神経伝達物質の遊離を増加させる[11]-[13]。

ニコチンは，VTAのDAニューロンに存在するα7 nAChRs[14][15]，およびVTAのDAニューロンにおけるシナプス前部のグルタミン酸作動性終末に存在するα7 nAChRs[16][17]に結合して活性化し，NAcでのDAの遊離を増加させる。ニコチンのα7 nAChRsへの親和性は，α4β2 nAChRsへの親和性と比べてはるかに低いので，ニコチンによる脱感作をそれほど受けない。そのためグルタミン酸遊離が増加することで，VTAのDAニューロンは長時間活性化し[18]，NAcの細胞外DAが長時間にわたって緩徐に増加する[19]。しかし興味深いことに，α7 nAChRsを欠損あるいは薬理学的に遮断しても，動物はニコチンと生理食塩水の区別(ニコチン弁別)ができるため，α7 nAChRsの活性化がニコチンによる報酬効果に関係していないことが示唆される[20]-[23]。

α3，α6，α7およびβ3を含む多くのnAChRsサブユニットがDA遊離に関与しているが，最近の研究では，α4β2 nAChRsがニコチンに対して依存性を形成するのに主要な役割を果たしていることが示唆されている。ヒトとげっ歯類を使用した試験では，脳切片標本にニコチンを慢性的に曝露すると，主にα4β2 nAChRsへのニコチン結合量が増加することが示された[24]。選択的α4β2 nAChRsアンタゴニスト，ジヒドロ-β-エリスロイジン(DHβE)または部分アゴニストSSR591813を前処置すると，ラットでのニコチン自己投与は有意に阻害される[25][26]。選択的α4β2 nAChRs部分アゴニストSSR591813あるいはα4サブユニットまたはβ2サブユニットの遺伝的欠損により，NAcでのニコチンによるDA遊離の増加が抑制される[26]-[28]。β2サブユニットの欠失により，NAcでのニコチンによるDA遊離の増加およびニコチンの自己投与は有意に減少するか，なくなる[27][29][30]。さらに，α4サブユニット・ノックアウトマウスまたはβ2サブユニット・ノックアウトマウスの脳切片標本には高親和性ニコチン結合がないので，α4β2 nAChRsがニコチンに対する強い結合部位であることが示唆される[26][31]。

ニコチンへの反復曝露によってα4β2 nAChRsの急速な脱感作がもたらされ，細胞表面のα4β2 nAChRsのアップレギュレーションが生じるが，ニコチンの除去によって脱感作はなくなる[32]-[35]。α4β2 nAChRsの脱感作用によるアップレギュレーションは，ニコチンに対する耐性やニコチンに対する依存性に関与する可能性がある。慢性喫煙者においては，α4β2 nAChRsが脱感作することによってニコチンを占有しなくなるため，ニコチン禁断症状時(夜間睡眠時)に機能が回復し，渇望症状および禁断症状が現れることが示唆されている[36]。したがって，起床後最初のタバコは，増加して十分に反応性のよくなったα4β2 nAChRsを刺激するため，最も強力な報酬効果を生み出すことを喫煙者は報告している[37]。

多くの喫煙者は，禁煙した際に不快な禁断症状を経験することを報告している。実験動物では，ニコチンの慢性投与を中断，またはnAChRs拮抗薬を投与すると身体的離脱症状を引き起こし，NAcにおけるDA遊離が減少した[38]。ニコチン投与の中止によって起こる身体的離脱症状は，回復する可能性がある[39]。したがって，喫煙に結びつくニコチンの禁断症状を解放することが，禁煙を促進する理想的な戦略

である。

前述したように，脱感による$\alpha4\beta2$ nAChRsの増加とニコチン結合を抑制することにより，NAcでのニコチンによるDA遊離が減少し，禁煙治療ができる可能性がある。理論的には，部分的な$\alpha4\beta2$ nAChRsアゴニストによる治療は，ニコチンの報酬効果を部分的に模倣することによってニコチン離脱の際の渇望症状および禁断症状を緩和するはずである。当然ながら，部分アゴニストは低い内因性機能的活性を有するため，受容体を完全に占有しても，完全アゴニストと比べて小さな最大作用を生み出す。さらに，高親和性$\alpha4\beta2$ nAChRs部分アゴニストは，$\alpha4\beta2$ nAChRsへのニコチンの結合を阻害し，拮抗作用を示す。前述した知見から，禁煙治療として，$\alpha4\beta2$ nAChRsサブタイプで部分アゴニストとして作用するリガンドの探索が促進された[40)41)]。$\alpha4\beta2$ nAChRsでの部分アゴニストとして，ファイザー社が開発したバレニクリンは禁煙の治療薬としてアメリカ食品医薬品局(FDA)によって承認されている。バレニクリンは，$\alpha4\beta2$ nAChRsに対して高親和性および高選択性を示し，受容体結合試験において他のnAChRsサブタイプ($\alpha3\beta4$および$\alpha7$-ホモマー受容体)やニコチン以外の受容体にはほとんど作用しないことが示されている[42)]。覚醒ラットのNAcにおいて，バレニクリンは，ニコチンと比べて40～70%少ないDA遊離を誘発するので，バレニクリンはニコチンより乱用の可能性が低いと考えられる[42)]。さらに，バレニクリンを前処理すると，NAcにおけるニコチンによるDA遊離の増加やニコチン自己投与が阻止される。一方，低用量のバレニクリンはそれ自身で報酬効果を示す[42)-44)]。バレニクリンの報酬効果は，選択的$\alpha7$ nAChRsアゴニストARR-17779ではなく，選択的$\alpha4\beta2$ nAChRsアゴニストSIB-1765Fに類似しており，選択的$\alpha7$ nAChRsアンタゴニストMLAではなく，選択的$\alpha4\beta2$ nAChRsアンタゴニストDHβEによって遮断されるので，バレニクリンの薬効は$\alpha4\beta2$ nAChRsを介している。したがって，バレニクリンは$\alpha4\beta2$ nAChRsを刺激して適度なレベルのDA遊離を維持し，禁煙期の渇望症状および禁断症状を軽減する。さらに，受容体拮抗作用により，再発の際に喫煙から得られるニコチンの報酬効果を遮断する。

臨床試験では常に，バレニクリンは喫煙の再発減少に有効であることが報告されている[45)46)]。直接比較では，アメリカの14ヵ所の治験実施施設で喫煙状況の12週治療期間および52週フォローアップによって行われた無作為化二重盲検プラセボ対照試験において，バレニクリンは禁煙達成についてプラセボや別の禁煙支援薬bupropionより優れた有効性を示した。52週目では，バレニクリン群における参加者の23%がプラセボ群の10.3%およびbupropion群の14.6%に比べて継続的に禁煙していた[47)]。日本人喫煙集団における無作為化二重盲検プラセボ対照並行群間試験において，バレニクリン投与により，最後の4週間の治療の間，そして非治療経過観察の40週以上のより長い期間での禁煙率が用量依存的に改善された[48)]。臨床試験でバレニクリンの治療は，鼻咽頭炎，悪心および頭痛のような有害事象により中止されているが，それらはすべて軽度または中等度である[47)-49)]。安全性に関する検討では，その前年に多種薬剤乱用歴がある45名の健康な成人喫煙者と非喫煙者を対象としたバレニクリン，amphetamine，プラセボの無作為化二重盲検ダブルダミープラセボ対照クロスオーバー比較実験において，バレニクリン乱用の可能性はプラセボと同様に低いと評価されている[50)]。

すべての利用可能な臨床試験結果は，バレニクリンが健康な成人喫煙者のニコチン離脱症状を緩和し，ニコチンによる報酬効果を低下させ禁煙を促進すること，また忍容性もあることから，禁煙の第一選択薬として推奨している。しかし，興奮，うつ病および自殺傾向を含む神経精神症状が市販後報告されたため，2008年初頭に海外で新しい安全警告が添付文書に追加された[51)]。しかしながら今日まで，バレニクリンの使用とこれらの症状の間の因果関係は証明されていない。今後は，一般集団，特に精神疾患のある喫煙群におけるバレニクリンの有効性および忍容性を確認するために，より多くの臨床試験と上市後のデータが必要である。

文　献

1）Hughes JR, Gulliver SB, Fenwick JW, et al：Smoking cessation among self-quitters. Health Psychol 1992；11：331-4.
2）Fiore MC, Pierce JP, Remington PL, et al：Cigarette smoking；the clinician's role in cessation, prevention, and public health. Dis Mon 1990；36：181-242.
3）Mansvelder HD, McGehee DS：Cel-

lular and synaptic mechanisms of nicotine addiction. J Neurobiol 2002 ; **53** : 606-17.
4) Wise RA : Dopamine, learning and motivation. Nat Rev Neurosci 2004 ; **5** : 483-94.
5) Corrigall WA, Coen KM, Adamson KL : Self-administered nicotine activates the mesolimbic dopamine system through the ventral tegmental area. Brain Res 1994 ; **653** : 278-84.
6) Corrigall WA : Nicotine self-administration in animals as a dependence model. Nicotine Tob Res 1999 ; **1** : 11-20.
7) Cooper E, Couturier S, Ballivet M : Pentameric structure and subunit stoichiometry of a neuronal nicotinic acetylcholine receptor. Nature 1991 ; **350** : 235-8.
8) Le Novère N, Grutter T, Changeux JP : Models of the extracellular domain of the nicotinic receptors and of agonist-and Ca2+-binding sites. Proc Natl Acad Sci U S A 2002 ; **99** : 3210-5.
9) Couturier S, Bertrand D, Matter JM, et al : A neuronal nicotinic acetylcholine receptor subunit (alpha 7) is developmentally regulated and forms a homo-oligomeric channel blocked by alpha-BTX. Neuron 1990 ; **5** : 847-56.
10) Zoli M, Léna C, Picciotto MR, et al : Identification of four classes of brain nicotinic receptors using beta2 mutant mice. J Neurosci 1998 ; **18** : 4461-72.
11) Zhu PJ, Chiappinelli VA : Nicotinic receptors mediate increased GABA release in brain through a tetrodotoxin-insensitive mechanism during prolonged exposure to nicotine. Neuroscience 2002 ; **115** : 137-44.
12) Lambe EK, Picciotto MR, Aghajanian GK : Nicotine induces glutamate release from thalamocortical terminals in prefrontal cortex. Neuropsychopharmacology 2003 ; **28** : 216-25.
13) Cao YJ, Surowy CS, Puttfarcken PS : Different nicotinic acetylcholine receptor subtypes mediating striatal and prefrontal cortical [3 H] dopamine release. Neuropharmacology 2005 ; **48** : 72-9.
14) Corrigall WA, Franklin KB, Coen KM, et al : The mesolimbic dopaminergic system is implicated in the reinforcing effects of nicotine. Psychopharmacology (Berl) 1992 ; **107** : 285-9.
15) Wu J, George AA, Schroeder KM, et al : Electrophysiological, pharmacological, and molecular evidence for alpha7-nicotinic acetylcholine receptors in rat midbrain dopamine neurons. J Pharmacol Exp Ther 2004 ; **311** : 80-91.
16) Yang K, Hu J, Lucero L, et al : Distinctive nicotinic acetylcholine receptor functional phenotypes of rat ventral tegmental area dopaminergic neurons. J Physiol 2009 ; **587** : 345-61.
17) Gass JT, Olive MF : Glutamatergic substrates of drug addiction and alcoholism. Biochem Pharmacol 2008 ; **75** : 218-65.
18) Mansvelder HD, McGehee DS : Long-term potentiation of excitatory inputs to brain reward areas by nicotine. Neuron 2000 ; **27** : 349-57.
19) Di Chiara G : Role of dopamine in the behavioural actions of nicotine related to addiction. Eur J Pharmacol 2000 ; **393** : 295-314.
20) Brioni JD, Kim DJ, O'Neill AB : Nicotine cue ; lack of effect of the alpha 7 nicotinic receptor antagonist methyllycaconitine. Eur J Pharmacol 1996 ; **301** : 1-5.
21) Gommans J, Stolerman IP, Shoaib M : Antagonism of the discriminative and aversive stimulus properties of nicotine in C57BL/6J mice. Neuropharmacology 2000 ; **39** : 2840-7.
22) Stolerman IP, Chamberlain S, Bizarro L, et al : The role of nicotinic receptor alpha7 subunits in nicotine discrimination. Neuropharmacology 2004 ; **46** : 363-71.
23) Zaniewska M, McCreary AC, Przegaliński E, et al : Evaluation of the role of nicotinic acetylcholine receptor subtypes and cannabinoid system in the discriminative stimulus effects of nicotine in rats. Eur J Pharmacol 2006 ; **540** : 96-106.
24) Marks MJ, Pauly JR, Gross SD, et al : Nicotine binding and nicotinic receptor subunit RNA after chronic nicotine treatment. J Neurosci 1992 ; **12** : 2765-84.
25) Watkins SS, Epping-Jordan MP, Koob GF, et al : Blockade of nicotine self-administration with nicotinic antagonists in rats. Pharmacol Biochem Behav 1999 ; **62** : 743-51.
26) Cohen C, Bergis OE, Galli F, et al : SSR591813, a novel selective and partial alpha4beta2 nicotinic receptor agonist with potential as an aid to smoking cessation. J Pharmacol Exp Ther 2003 ; **306** : 407-20.
27) Picciotto MR, Zoli M, Rimondini R, et al : Acetylcholine receptors containing the beta2 subunit are involved in the reinforcing properties of nicotine. Nature 1998 ; **391** : 173-7.
28) Marubio LM, Gardier AM, Durier S, et al : Effects of nicotine in the dopaminergic system of mice lacking the alpha 4 subunit of neuronal nicotinic acetylcholine receptors. Eur J Neurosci 2003 ; **17** : 1329-37.
29) Grady SR, Meinerz NM, Cao J, et al : Nicotinic agonists stimulate acetylcholine release from mouse interpeduncular nucleus ; a function mediated by a different nAChR than

dopamine release from striatum. J Neurochem 2001 ; **76** : 258-68.
30) Shoaib M, Gommans J, Morley A, et al : The role of nicotinic receptor beta-2 subunits in nicotine discrimination and conditioned taste aversion. Neuropharmacol 2002 ; **42** : 530-9.
31) Picciotto MR, Zoli M, Lena C, et al : Abnormal avoidance learning in mice lacking functional high-affinity nicotine receptor in the brain. Nature 1995 ; **374** : 65-7.
32) Wooltorton JR, Pidoplichko VI, Broide RS, et al : Differential desensitization and distribution of nicotinic acetylcholine receptor subtypes in midbrain dopamine areas. J Neurosci 2003 ; **23** : 3176-85.
33) Peng X, Gerzanich V, Anand R, et al : Nicotine-induced increase in neuronal nicotinic receptors results from a decrease in the rate of receptor turnover. Mol Pharmacol 1994 ; **46** : 523-30.
34) Fenster CP, Hicks JH, Beckman ML, et al : Desensitization of nicotinic receptors in the central nervous system. Ann N Y Acad Sci 1999 ; **868** : 620-3.
35) Buisson B, Bertrand D : Chronic exposure to nicotine upregulates the human (alpha) 4 (beta) 2 nicotinic acetylcholine receptor function. J Neurosci 2001 ; **21** : 1819-29.
36) Dani JA, Heinemann S : Molecular and cellular aspects of nicotine abuse. Neuron 1996 ; **16** : 905-8.
37) Russell MA : Subjective and behavioural effects of nicotine in humans ; some sources of individual variation. Prog Brain Res 1989 ; **79** : 289-302.
38) Hildebrand BE, Nomikos GG, Hertel P, et al : Reduced dopamine output in the nucleus accumbens but not in the medial prefrontal cortex in rats displaying a mecamylamine-precipitated nicotine withdrawal syndrome. Brain Res 1998 ; **779** : 214-25.
39) Epping-Jordan MP, Watkins SS, Koob GF, et al : Dramatic decreases in brain reward function during nicotine withdrawal. Nature 1998 ; **393** : 76-9.
40) Foulds J : The neurobiological basis for partial agonist treatment of nicotine dependence ; varenicline. Int J Clin Pract 2006 ; **60** : 571-6.
41) Mihalak KB, Carroll FI, Luetje CW : Varenicline is a partial agonist at alpha4beta2 and a full agonist at alpha7 neuronal nicotinic receptors. Mol Pharmacol 2006 ; **70** : 801-5.
42) Coe JW, Brooks PR, Vetelino MG, et al : Varenicline ; an alpha4beta2 nicotinic receptor partial agonist for smoking cessation. J Med Chem 2005 ; **48** : 3474-7.
43) Rollema H, Chambers LK, Coe JW, et al : Pharmacological profile of the alpha4beta2 nicotinic acetylcholine receptor partial agonist varenicline, an effective smoking cessation aid. Neuropharmacol 2007 ; **52** : 985-94.
44) Spiller K, Xi ZX, Li X, et al : Varenicline attenuates nicotine-enhanced brain-stimulation reward by activation of alpha4beta2 nicotinic receptors in rats. Neuropharmacol 2009 ; **57** : 60-6.
45) Zierler-Brown SL, Kyle JA : Oral varenicline for smoking cessation. Ann Pharmacother 2007 ; **41** : 95-9.
46) Tutka P : Nicotine receptor partial agonists as novel compounds for the treatment of smoking cessation. Expert Opin Investig Drugs 2008 ; **17** : 1473-85.
47) Jorenby DE, Hays JT, Rigotti NA, et al ; Varenicline Phase 3 Study Group : Efficacy of varenicline, an alpha4beta2 nicotinic acetylcholine receptor partial agonist, vs placebo or sustained-release bupropion for smoking cessation ; a randomized controlled trial. JAMA 2006 ; **296** : 56-63.
48) Nakamura M, Oshima A, Fujimoto Y, et al : Efficacy and tolerability of varenicline, an alpha4beta2 nicotinic acetylcholine receptor partial agonist, in a 12-week, randomized, placebo-controlled, dose-response study with 40-week follow-up for smoking cessation in Japanese smokers. Clin Ther 2007 ; **29** : 1040-56.
49) Garrison GD, Dugan SE : Varenicline ; a first-line treatment option for smoking cessation. Clin Ther 2009 ; **31** : 463-91.
50) McColl SL, Burstein AH, Reeves KR, et al : Human abuse liability of the smoking cessation drug varenicline in smokers and nonsmokers. Clin Pharmacol Ther 2008 ; **83** : 607-14.
51) Hays JT, Ebbert JO, Sood A : Efficacy and safety of varenicline for smoking cessation. Am J Med 2008 ; **121** : S32-42.

Tursun Alkam
平成20年 名古屋大学大学院医学研究科博士課程修了
現在，名城大学大学院薬学研究科薬品作用学教室博士研究員
専門分野：神経精神薬理学
E-mail：alkam@ccmfs.meijo-u.ac.jp

International Journal of Neuropsychopharmacology, Page 1 of 13. Copyright © CINP 2009
doi:10.1017/S1461145709990757

ARTICLE

CINP

Prenatal exposure to phencyclidine produces abnormal behaviour and NMDA receptor expression in postpubertal mice

Lingling Lu[1,2], Takayoshi Mamiya[1], Ping Lu[1,2], Kazuya Toriumi[1], Akihiro Mouri[1,4], Masayuki Hiramatsu[1], Hyoung-Chun Kim[5], Li-Bo Zou[2], Taku Nagai[3] and Toshitaka Nabeshima[1,6]

[1] *Department of Chemical Pharmacology, Graduate School of Pharmaceutical Sciences, Meijo University, Nagoya, Japan*
[2] *Department of Pharmacology, School of Life Science and Biopharmaceutics, Shenyang Pharmaceutical University, Shenyang, China*
[3] *Department of Neuropsychopharmacology and Hospital Pharmacy, Nagoya University Graduate School of Medicine, Nagoya, Japan*
[4] *Division of Scientific Affairs, Japanese Society of Pharmacopoeia, Tokyo, Japan*
[5] *Neuropsychopharmacology and Toxicology Program, College of Pharmacy, Kangwon National University, Chunchon, South Korea*
[6] *Japanese Drug Organization of Appropriate Use and Research, Nagoya, Japan*

Abstract

Several studies have shown the disruptive effects of non-competitive *N*-methyl-D-aspartate (NMDA) receptor antagonists on neurobehavioural development. Based on the neurodevelopment hypothesis of schizophrenia, there is growing interest in animal models treated with NMDA antagonists at developing stages to investigate the pathogenesis of psychological disturbances in humans. Previous studies have reported that perinatal treatment with phencyclidine (PCP) impairs the development of neuronal systems and induces schizophrenia-like behaviour. However, the adverse effects of prenatal exposure to PCP on behaviour and the function of NMDA receptors are not well understood. This study investigated the long-term effects of prenatal exposure to PCP in mice. The prenatal PCP-treated mice showed hypersensitivity to a low dose of PCP in locomotor activity and impairment of recognition memory in the novel object recognition test at age 7 wk. Meanwhile, the prenatal exposure reduced the phosphorylation of NR1, although it increased the expression of NR1 itself. Furthermore, these behavioural changes were attenuated by atypical antipsychotic treatment. Taken together, prenatal exposure to PCP produced long-lasting behavioural deficits, accompanied by the abnormal expression and dysfunction of NMDA receptors in postpubertal mice. It is worth investigating the influences of disrupted NMDA receptors during the prenatal period on behaviour in later life.

Received 10 March 2009; Reviewed 6 April 2009; Revised 7 August 2009; Accepted 28 August 2009

Key words: Antipsychotic, behaviour, neurodevelopment, NMDA receptor, PCP, prenatal.

Introduction

Neurodevelopmental abnormalities are considered part of the pathogenesis of psychological disturbances. Exposure to environmental insults during pregnancy increases the probability of neuropsychiatric disorders in later life (Brown & Susser, 2002; Green *et al.* 1994). According to the neurodevelopmental hypothesis of schizophrenia, disruption of the prenatal brain predisposes the neural systems to long-lasting structural and functional abnormalities, leading to the emergence of psychopathological behaviour in adulthood (Ashdown *et al.* 2006).

The *N*-methyl-D-aspartate (NMDA) receptor, a kind of ligand-gated ion channel, is a heteromeric assembly comprising a core NR1 subunit and several modulatory subunits. At the cell surface, including synapses, NMDA receptors are anchored and clustered forming larger complexes (Husi & Grant, 2001). Stimulation of NMDA receptors during development

Address for correspondence to: T. Nabeshima, Ph.D., Department of Chemical Pharmacology, Graduate School of Pharmaceutical Sciences, Meijo University, 150 Yagotoyama, Tempaku-ku, Nagoya 468-8503, Japan.
Tel.: +81-52-839-2735 *Fax*: +81-52-839-2738.
Email: tnabeshi@ccmfs.meijo-u.ac.jp

is critical for the survival, differentiation and migration of immature neurons (Behar *et al.* 1999; Komuro & Rakic, 1993), and controls structure and plasticity (Scheetz & Constantine-Paton, 1994), as well as establishing normal neural networks in the developing brain (Deutsch *et al.* 1998). It has been found that pharmacological inhibition of NMDA receptors during development disturbs neural functions in the brain (Bellinger *et al.* 2002). Post-mortem studies have identified the abnormal expression (Akbarian *et al.* 1996; Dracheva *et al.* 2001) and phosphorylation (Emamian *et al.* 2004) of NMDA receptors in the prefrontal cortex (PFC) of schizophrenia patients.

In clinical tests, abuse of phencyclidine (PCP), a non-competitive NMDA receptor antagonist, causes a schizophrenic psychosis in normal volunteers and exacerbates symptoms in schizophrenia patients (Javitt & Zukin, 1991). In adult rodents, PCP produces abnormal behaviour and biochemical alterations resembling schizophrenia including positive symptoms, negative symptoms, and cognitive deficits (Mouri *et al.* 2007*a*,*c*; Noda *et al.* 1995). However, several lines of evidence suggest that abnormal architectural arrangements of nerve cells, or cortical layers (Bogerts, 1993), an absence of normal cerebral structural asymmetry (Crow *et al.* 1989), and gliosis (Jones *et al.* 1994) are involved in the pathology of schizophrenia. This suggests schizophrenia to be a developmental disorder rather than a progressive degenerative disease (Bogerts, 1993).

Therefore, although many schizophrenia-like symptoms are observed in adult rodents repeatedly treated with PCP, it is unlikely that these abnormalities completely resemble the pathogenesis of schizophrenia, since at least in some cases, they occur in the developing period initiated by prenatal insults (Murray *et al.* 1992; Pilowski *et al.* 1993). Therefore, based on the neurodevelopmental hypothesis, several studies have modified this classic 'PCP animal model', through treatment with NMDA antagonists early in the development of the brain. For instance, perinatal PCP treatment in rats enhanced hyperlocomotion elicited by PCP and impaired the acquisition of a delayed spatial alternation task in adolescent offspring, associated with the disruption of neurodevelopment (Deutsch *et al.* 1998; Wang *et al.* 2001). Prenatal exposure to (+)-MK-801 has been reported to reduce the density of parvalbumin-immunoreactive interneurons and enhance PCP-induced hyperlocomotion in postpubertal rats (Abekawa *et al.* 2007). However, it is unclear whether prenatal exposure to PCP leads to behavioural and NMDA receptor dysfunction in mice.

In this study, we investigated the influences of prenatal exposure to PCP during the middle and late stages of pregnancy [embryonic days 6–18 (E6–E18)], covering the entire neurodevelopment period in the prenatal brain from neurulation to corticogenesis (Theiler, 1989). PCP-induced hyperlocomotion, recognition memory, and the expression and phosphorylation of NR1 protein were investigated from age 7 wk. In addition, the effects of antipsychotics on these behavioural abnormalities were further evaluated.

Materials and methods

Animals

Pregnant ICR dams (E5) obtained from SLC Japan (Shizuoka, Japan) were maintained on a 12-h light/dark cycle (lights on 08:00 hours) with free access to food (CE2; Clea Japan Inc., Japan) and water. The dams were randomly divided into saline-treated and PCP-treated groups. All were housed individually until parturition. There was no increase in maternal deaths and resorption or stillbirths on exposure to PCP in this study. At birth [postnatal day 0 (PD 0)], pups were culled to eight per litter with a balance of males and females wherever possible. Pups were weighed weekly until weaning and maternal care behaviour during feeding was monitored. After weaning at PD 21, pups given the same prenatal treatment were mixed by gender and then randomly assigned to each group for behavioural testing at the age of 7–8 wk. All groups of mice had litters of 2–3 and the test was repeated more than three times to reduce the influence of litters. Moreover, a balanced number of males and females were used in each experiment, since there were no significant differences between genders in this study.

The experiments with offspring commenced at the age of 7 wk and were performed in a sound-attenuated, air-conditioned room (23 ± 1 °C, 50 ± 5% humidity). The mice were habituated to the room for 40 min before the behavioural experiments. All the behavioural tests were recorded with a digital camera to re-analyse the results. The experiments were performed in accordance with the Guidelines for Animal Experiments of Meijo University Faculty of Pharmaceutical Sciences and the Guiding Principles for the Care and Use of Laboratory Animals approved by the Japanese Pharmacological Society (2008).

Drugs

PCP hydrochloride was synthesized according to the method of Maddox *et al.* (1965) and checked for purity.

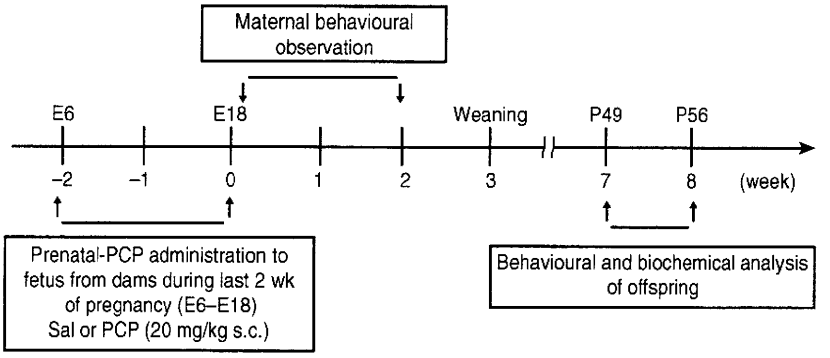

Fig. 1. Experimental protocol of this study.

The PCP was dissolved in saline prior to use. Clozapine (Sigma, USA) was dissolved in a minimum amount of 0.1 N HCl and then diluted with saline (adjusted to pH 6–7 with 0.1 N NaOH), as previously described (Qiao *et al.* 2001). An injectable solution of haloperidol (5 mg/ml; Tanabe Seiyaku, Japan) was diluted with saline. All compounds were administered in a volume of 0.1 ml/10 g body weight.

Drug treatment

The dams were administered saline or PCP (20 mg/kg s.c.) once daily at 18:00 hours on E6–E18. The injection was made as gentle as possible to minimize potential stress-related influences on dams. In the fetal brain, the density of NMDA receptors is relatively low (Monyer *et al.* 1994; Watanabe *et al.* 1992), and the affinity for PCP, as well as the distribution of PCP, remains unclear. According to dose-dependent responses in our preliminary study (2.5–20 mg/kg), the dose of 20 mg/kg was selected in the present study, since it produced more obvious and similar behavioural and biochemical changes in relation to schizophrenia (L. Lu *et al.*, unpublished data).

Based on previous studies (Mouri *et al.* 2007*a*), a low dose of PCP (3 mg/kg) or saline was used to challenge mice 30 min after habituation in PCP-induced locomotion; clozapine (1 and 3 mg/kg) or haloperidol (0.1 and 0.3 mg/kg) were injected 30 min before each behavioural test, and PCP (3 mg/kg) was injected into all mice to evaluate the effects of antipsychotics on it.

Different batches of mice were used for different experiments to avoid disruption. The experiments were performed according to the protocol shown in Fig. 1.

Measurement of locomotor activity

Locomotor activity was measured at the age of 7 wk. Mice were placed individually in a transparent acrylic cage with a black frosted Plexiglas floor (45 × 26 × 40 cm) for 120 min, and locomotor activity was measured in 5-min intervals using digital counters with infrared sensors (Scanet SV-10; Melquest Ltd, Japan) as previously reported (Lu *et al.* 2009). Locomotor activity was defined as the total number of beam cuts due to horizontal movement measured by the photo sensors.

Novel object recognition test (NORT)

As previously described (Mouri *et al.* 2007*b*), the test procedure consisted of three sessions: habituation, training, and retention. Each mouse was individually habituated to the box (L 30 × W 30 × H 35 cm), with 10 min of exploration in the absence of objects for 3 d (habituation session). During the training session, two objects (a red painted triangular prism and a yellow painted quadratic prism) were symmetrically fixed to the floor of the box, 8 cm from the walls, and each animal was allowed to explore the box for 10 min (day 4). An animal was considered to be exploring the object when its head was facing the object or it was touching or sniffing the object at a distance of <2 cm and/or touching it with its nose. The time spent exploring each object was recorded. After training, mice were immediately returned to their home cages. During the retention session, animals were returned to the same box 24 h (day 5) after the training session, in which one of the familiar objects used during training was replaced with a novel object (a black painted golf ball). The animals were allowed to explore freely for 5 min and the time spent exploring each object was recorded. Throughout the experiments, the objects were used in a counterbalanced manner in terms of their physical complexity and emotional neutrality. A preference index, the ratio of time spent exploring either of the two objects (training session) or the novel object (retention session) over the total amount of time

spent exploring both objects, was used to assess cognitive function.

Western blot analysis

Western blotting was performed as previously described (Mouri *et al.* 2007*c*). Dissected brain tissue obtained 24 h after the NORT test, was homogenized in ice-cold Tris buffer A [10 mM Tris–HCl (pH 7.4), 5 mM EDTA, 320 mM sucrose, 1 mM EGTA, 0.1 mM sodium orthovanadate, 1 mM NaF, 5 μg/ml aprotinin, 5 μg/ml leupeptin, and 5 μg/ml pepstatin] and centrifuged at 700 *g* for 10 min. The supernatant was centrifuged again at 37 000 *g* for 40 min, and the membrance-enriched extracts were re-suspended in Tris buffer B [10 mM Tris–HCl (pH 7.4), 0.1 mM sodium orthovanadate, 1 mM NaF, 5 μg/ml aprotinin, 5 μg/ml leupeptin, and 5 μg/ml pepstatin], and the suspension was used.

The protein concentrations were determined using a Pierce BCA Protein Assay kit (Thermo, USA). Samples were boiled at 95 °C for 5 min in the sample buffer [125 mM Tris–HCl (pH 6.8), 10% 2-mercaptoethanol, 4% sodium diphosphate decahydrate, 10% sucrose, and 0.0004% Bromophenol Blue], separated on a polyacrylamide gel, and transferred to polyvinylidene difluoride membranes (Millipore Corporation, USA). The membranes were blocked with a Detector Block kit (Kirkegaard & Perry Laboratories, USA) and probed with a primary antiphospho-NR1 (Ser^{897}) antibody (1:1000; Upstate Biotechnology, USA). Membranes were washed with the washing buffer [50 mM Tris–HCl (pH 7.4), 0.05% Tween-20, and 150 mM NaCl] and subsequently incubated with a secondary horseradish peroxidase-linked antibody (Kirkegaard & Perry Laboratories). The immune complexes were detected with an ECL kit (GE Healthcare, UK) and exposed to X-ray film (Hyperfilm, GE Healthcare). The intensity of bands was analysed by Atto Densitogram Software Library Lane Analyzer (Atto, Japan). After the phosphorylated-NR1 was detected, membranes were stripped with stripping buffer (100 mM 2-mercaptoethanol, 2% SDS, and 62.5 mM Tris–HCl, pH 6.7) at 50 °C for 30 min, and NR1 expression was detected with a primary anti-NR1 antibody (1:1000; Santa Cruz Biotechnology, USA).

Preparation of brain slices and staining

Histological procedures were performed as described with a minor modification (Murai *et al.* 2007). Mice were anaesthetized with pentobarbital sodium (50 mg/kg i.p.) and perfused transcardially with ice-cold phosphate-buffered saline (PBS), followed by 4% paraformaldehyde and then soaked in 10–30% (w/v) sucrose. Coronal sections (20-μm thick) were cut with a cryostat (CM 1850; Leica, Germany). According to a previous method (Shen *et al.* 2008), Cresyl Violet staining was performed and the sizes of ventricles and brains were quantified with a computer-based image analysis system (WinRoof, Mitani, Japan). Apoptosis was detected with an *in-situ* cell-death detection kit, POD (Roche, Germany), and TUNEL-positive cells in layers II/III of the prelimbic area were counted using image analysis software. Images were acquired with a microscope (BZ-9000; Keyence, Japan).

Statistical analysis

All data were expressed as the mean ± S.E.M. The statistical significance of differences between two groups was determined by Student's *t* test. The significance of differences among more than three groups was determined using a two-way analysis of variance (ANOVA) or ANOVA with repeated measures, followed by Bonferroni's test. Pearson's correlation analysis was used to identify the relationship; $p<0.05$ was regarded as statistically significant.

Results

Effect of prenatal-PCP treatment on PCP-induced hyperlocomotion

To investigate the effects of prenatal exposure to PCP on drug-induced sensitization, PCP-induced hyperlocomotion was examined at age 7 wk. In the habituation period, no significant differences were observed among groups. After the 30-min habituation, prenatal saline- or PCP-treated mice were administered a low dose of PCP (3 mg/kg) or saline. The time-course of change in prenatal saline-treated mice revealed that the PCP challenge rapidly and significantly increased locomotion compared to the administration of saline. PCP-induced hyperlocomotion was significantly potentiated in the prenatal PCP-treated mice compared to the prenatal saline-treated mice over 5-min intervals after habituation (prenatal treatment: $F_{1,37}=9.54$, $p<0.01$; PCP challenge: $F_{1,37}=64.85$, $p<0.01$; prenatal treatment × PCP challenge: $F_{1,37}=5.73$, $p<0.05$; time: $F_{17,629}=45.82$, $p<0.01$; time × prenatal treatment: $F_{17,629}=2.33$, $p<0.01$; time × PCP challenge: $F_{17,629}=20.20$, $p<0.01$; time × prenatal treatment × PCP challenge: $F_{17,629}=1.13$, $p>0.05$, repeated two-way ANOVA; Fig. 2*a*), and the entire 90 min (30–120 min) ($F_{\text{group}(1,37)}=9.20$, $p<0.01$; $F_{\text{treatment}(1,37)}=65.19$, $p<0.01$; $F_{\text{group}\times\text{treatment}(1,37)}=5.73$, $p<0.05$, two-way ANOVA; Fig. 2*b*).

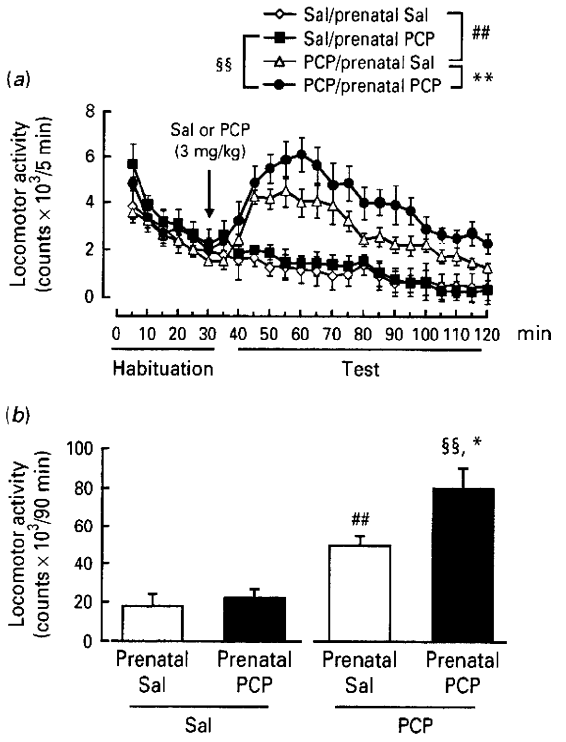

Fig. 2. Effect of prenatal phencyclidine (PCP) treatment on PCP-induced hyperlocomotion. PCP (3 mg/kg) or saline (Sal) was administered after 30 min of habituation. The locomotor activity of mice was assessed over 5-min intervals during the last 90 min after habituation (prenatal treatment: $F_{1,37}=9.54$, $p<0.01$; PCP challenge: $F_{1,37}=64.85$, $p<0.01$; prenatal treatment × PCP challenge: $F_{1,37}=5.73$, $p<0.05$; time: $F_{17,629}=45.82$, $p<0.01$; time × prenatal treatment: $F_{17,629}=2.33$, $p<0.01$; time × PCP challenge: $F_{17,629}=20.20$, $p<0.01$; time × prenatal treatment × PCP challenge: $F_{17,629}=1.13$, $p>0.05$, repeated two-way ANOVA) (*a*) and the entire 90 min (30–120 min) ($F_{\text{group}(1,37)}=9.20$, $p<0.01$; $F_{\text{treatment}(1,37)}=65.19$, $p<0.01$; $F_{\text{group}\times\text{treatment}(1,37)}=5.73$, $p<0.05$, two-way ANOVA) (*b*). $^{\#\#}p<0.01$ compared to Sal/prenatal Sal group. $^{*}p<0.05$, $^{**}p<0.01$ compared to PCP/prenatal Sal group. $^{\S\S}p<0.01$ compared to Sal/prenatal PCP group. Data are expressed as the mean ± S.E.M. for 10–11 mice (Bonferroni's test).

Effect of prenatal-PCP treatment on cognitive function in the NORT

To investigate the effects of prenatal PCP treatment on cognitive function, recognition memory was evaluated in the NORT. In the training session, the prenatal saline- or PCP-treated mice spent equal amounts of time exploring either of the two objects, and there was no biased exploratory preference in each group (prenatal saline-treated mice, 50.4±1.7%; prenatal PCP-treated mice, 53.6±2.6%; $p>0.05$, Fig. 3*a*). In addition, the total time spent in exploration of objects in the training session did not differ between these two groups (prenatal saline-treated mice, 28.3±2.7 s; prenatal PCP-treated mice, 32.0±3.7 s; $p>0.05$, Fig. 3*b*). However, when retention performance was tested, the prenatal PCP-treated mice showed a reduced level of exploratory preference for the novel objects compared to the prenatal saline-treated group (prenatal saline-treated mice, 70.6±2.1%; prenatal PCP-treated mice, 54.5±2.9%; $p<0.01$, Fig. 3*c*). There was no significant difference in total exploration time in the retention session (prenatal saline-treated mice, 17.4±2.3 s; prenatal PCP-treated mice, 16.6±2.3 s; $p>0.05$, Fig. 3*d*).

The sizes of lateral ventricles and brain in prenatal PCP-treated mice

We examined whether prenatal exposure to PCP induced any architectural abnormalities of lateral ventricles and brain at age 7 wk. However, there were no obvious differences between the prenatal saline- and PCP-treated mice in the ratio of brain to body weight (prenatal saline-treated mice, 6.12±0.15%; prenatal PCP-treated mice, 6.02±0.17%; $p>0.05$, Supplementary Fig. S2*e*, available online), the size of lateral ventricles (prenatal treatment: $F_{1,6}=1.93$, $p>0.05$; bregma: $F_{3,18}=493.88$, $p<0.01$; prenatal treatment × bregma: $F_{3,18}=0.85$, $p>0.05$, repeated one-way ANOVA; Suppl. Fig. S2*f*) and of whole brain (prenatal treatment: $F_{1,6}=0.25$, $p>0.05$; bregma: $F_{3,18}=4.44$, $p<0.05$; prenatal treatment × bregma: $F_{3,18}=0.14$, $p>0.05$, repeated one-way ANOVA; Suppl. Fig. S2*g*), as well as the ratio of lateral ventricles to brain size (prenatal treatment: $F_{1,6}=3.93$, $p>0.05$; bregma: $F_{3,18}=564.37$, $p<0.01$; prenatal treatment × bregma: $F_{3,18}=1.98$, $p>0.05$, repeated one-way ANOVA; Suppl. Fig. S2*h*). These suggested the architecture of lateral ventricles was not affected by the prenatal treatment.

Changes in the expression and phosphorylation of the NR1 subunit of NMDA receptors of prenatal PCP-treated mice

We postulated that the abnormal behaviour was accompanied by a malfunction of NMDA receptors, since PCP as a non-competitive NMDA antagonist might inhibit NMDA receptors during development. The level of NR1 protein was significantly increased in the prenatal PCP-treated mice compared to that in the prenatal saline-treated mice (PFC: 100.0±7.6% *vs.* 152.0±12.9%; $p<0.01$, Fig. 4*a*; hippocampus: 100.0±10.8% *vs.* 140.9±12.2%; $p<0.05$, Fig. 5*e*; striatum: 100.0±10.9% *vs.* 138.3±10.8%; $p<0.05$, Fig. 4*i*). In contrast, the level of NR1 phosphorylated at Ser^{897} was

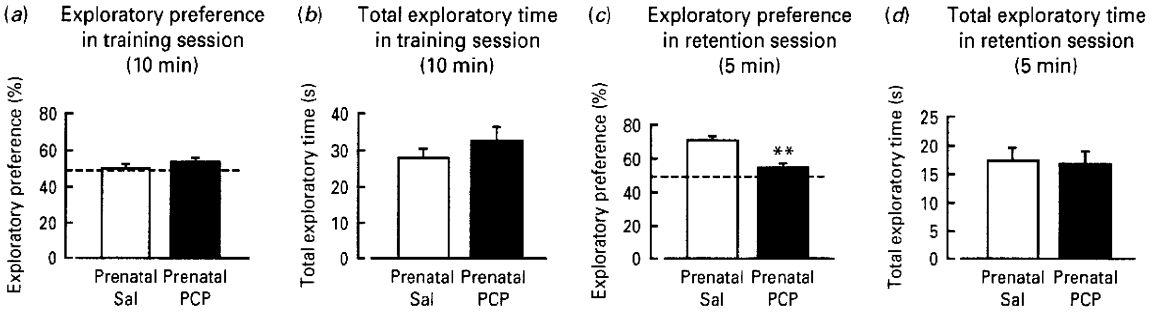

Fig. 3. Effect of prenatal phencyclidine (PCP) treatment on cognitive function in the novel object recognition test. Exploratory preference in (*a*) the training session and (*c*) the retention session. Total time spent exploring the objects in (*b*) the training session and (*d*) the retention session. ** $p<0.01$ compared to the prenatal saline (Sal) group. Data are expressed as the mean ± S.E.M. for 11–12 mice (Student's *t* test).

decreased in prenatal PCP-treated mice (PFC: 100.0 ± 5.9% *vs.* 75.4 ± 7.1%; $p<0.05$, Fig. 4*b*; hippocampus: 100.0 ± 10.5% *vs.* 67.8 ± 9.5%; $p<0.05$; Fig. 4*f*; striatum: 100.0 ± 7.3% *vs.* 87.1 ± 10.1%; $p>0.05$, Fig. 4*j*). Furthermore, the proportion of phosphorylated-NR1 was also significantly reduced in prenatal PCP-treated mice (PFC: 100.0 ± 8.5% *vs.* 50.1 ± 6.7%; $p<0.01$, Fig. 4*c*; hippocampus: 100.0 ± 13.4% *vs.* 48.8 ± 10.5%; $p<0.05$, Fig. 4*g*; striatum: 100.0 ± 14.3% *vs.* 55.0 ± 5.8%; $p<0.05$, Fig. 4*k*). Moreover, between the cognitive deficit in the NORT and the decreased level of phosphorylated NR1, there was a significant correlation in the PFC ($r=0.587$, $p=0.045$, Pearson's correlation; Fig. 4*d*), and a positive and almost significant correlation in the hippocampus ($r=0.569$, $p=0.054$, Pearson's correlation; Fig. 4*h*), but no correlation in the striatum ($r=0.325$, $p>0.05$, Pearson's correlation; Fig. 4*l*).

However, a lower dose of prenatal PCP exposure (5 mg/kg) did not affect the expression of phosphorylated NR1 in the PFC of postpubertal mice (100 ± 4.23% *vs.* 91.41 ± 6.69%; $p>0.05$, Suppl. Fig. S3). Additionally, the behavioural test itself did not affect the expression or phosphorylation of NR1 ($p>0.05$, Suppl. Fig. S4).

The neurotoxicity of prenatal-PCP treatment in the developing brain

To evaluate the neurotoxic effects of prenatal PCP treatment during neurodevelopment, the TUNEL-positive cells in the PFC were counted at PD 0, PD 7 and PD 49. As shown by the results, apoptosis was significantly increased at PD 0 (253.4 ± 19.9 *vs.* 338.8 ± 28.2; $p<0.05$, Suppl. Fig. S1*a*, *d*), but was not observed at either PD 7 (31.5 ± 3.9 *vs.* 37.2 ± 3.5; $p>0.05$, Suppl. Fig. S1*b*, *e*), or PD 49 (35.7 ± 5.1 *vs.* 39.1 ± 4.0; $p>0.05$, Suppl. Fig. S1*c*, *f*).

Effect of antipsychotics on the behavioural abnormalities in prenatal PCP-treated mice

We evaluated whether the prenatal PCP-induced behavioural changes were sensitive to both the atypical antipsychotic clozapine (Clz) and the typical antipsychotic haloperidol (Hal). The results showed that clozapine selectively attenuated the PCP-induced hypersensitivity over the 5-min intervals after habituation (30–120 min) in the prenatal PCP-treated mice (prenatal treatment: $F_{1,62}=15.41$, $p<0.01$; Clz: $F_{2,62}=29.07$, $p<0.01$; prenatal treatment × Clz: $F_{2,62}=5.23$, $p<0.01$; time: $F_{\text{time}(17,1054)}=70.46$, $p<0.01$; time × prenatal treatment: $F_{17,1054}=1.96$, $p<0.05$; time × Clz: $F_{34,1054}=3.03$, $p<0.01$; time × prenatal treatment × Clz: $F_{34,1054}=1.05$, $p>0.05$, repeated two-way ANOVA; Fig. 5*a*). However, haloperidol reduced the hyperlocomotion of mice in both the prenatal saline- and PCP-treated groups (prenatal treatment: $F_{1,63}=6.88$, $p<0.05$; Hal: $F_{2,63}=17.35$, $p<0.01$; prenatal treatment × Hal: $F_{2,63}=1.30$, $p>0.05$; time: $F_{\text{time }17,1071}=29.46$, $p<0.01$; time × prenatal treatment: $F_{17,1071}=1.66$, $p<0.05$; time × Hal: $F_{34,1071}=3.15$, $p<0.01$; time × prenatal treatment × Hal: $F_{34,1071}=0.92$, $p>0.05$, repeated two-way ANOVA; Fig. 5*c*). Furthermore, in terms of the entire 120-min period, the higher dose of clozapine (3 mg/kg) and haloperidol (0.1 and 0.3 mg/kg) reduced the locomotion in both the first 30 min and the last 90 min (Clz: 0–30 min: $F_{\text{group}(1,62)}=3.23$, $p>0.05$; $F_{\text{treatment}(2,62)}=5.98$, $p<0.01$; $F_{\text{group}\times\text{treatment}(2,62)}=0.12$, $p>0.05$, two-way ANOVA; 30–120 min: $F_{\text{group}(1,62)}=14.84$, $p<0.01$; $F_{\text{treatment}(2,62)}=29.07$, $p<0.01$; $F_{\text{group}\times\text{treatment}(2,62)}=5.23$, $p<0.01$, two-way ANOVA; Fig. 5*b*; Hal: 0–30 min: $F_{\text{group}(1,63)}=1.23$, $p>0.05$; $F_{\text{treatment}(2,63)}=14.90$, $p<0.01$; $F_{\text{group}\times\text{treatment}(2,63)}=0.56$, $p>0.05$, two-way ANOVA; 30–120 min: $F_{\text{group}(1,63)}=7.43$, $p<0.01$; $F_{\text{treatment}(2,63)}=17.28$, $p<0.01$; $F_{\text{group}\times\text{treatment}(2,63)}=1.30$, $p>0.05$, two-way